Bull. Natl. Mus. Nat. Sci., Ser. D, 38, pp. 1–37, November 22, 2012

Possible Causes of Three-Dimensional Structural Deviations in the Neighborhood of Cranial Landmarks: Occlusal Force and Aging

Yuji Mizoguchi

Department of Anthropology, National Museum of Nature and Science
4–1–1 Amakubo, Tsukuba, Ibaraki 305–0005, Japan
E-mail: mzgch@kahaku.go.jp

Abstract To seek the causes of three-dimensional morphological variations in the human skull, correlations between the 3D structural deviations in the neighborhood of cranial landmarks obtained by the finite element scaling method and the degree of dental wear or age were examined by principal component analysis using three male adult samples from Japanese, Indians, and African-Americans. The results showed that the degree of dental wear is positively associated with the magnitude of strain at the inion in Japanese; that dental wear is inversely associated with the magnitude of strain at the frontotemporale in Japanese; and that age is positively associated with the magnitude of strain at the center of the parietal tuber in African-Americans. These significant associations suggest, at least, that the craniofacial form varies along with age even in adulthood and, possibly, also in response to mechanical stresses from the masticatory and/or nuchal muscles.
Key words: Human cranial form, Three-dimensional coordinates, Finite element scaling analysis, Dental wear, Age

In recent years, with the development of apparatus and software for capturing and analyzing three-dimensional (3D) coordinates, many geometric morphometric (Marcus *et al.*, 1996) studies have been carried out in the field of physical anthropology. Although most of them were based on the generalized Procrustes analysis (e.g., Detroit, 2000; Bookstein, 1991; Hennessy and Stringer, 2002; Bookstein *et al.*, 2003; Harvati, 2003; Slice, 2005; Gunz and Harvati, 2007; Gunz *et al.*, 2009; Hublin *et al.*, 2009; Makishima and Ogihara, 2009; Bigoni *et al.*, 2010; Fukumoto and Kondo, 2010; Harvati *et al.*, 2010; Neubauer *et al.*, 2010; Williams and Slice, 2010; Bienvenu *et al.*, 2011; Coquerelle *et al.*, 2011; Gonzalez *et al.*, 2011; Noback *et al.*, 2011; von Cramon-Taubadel, 2011; Weisensee and Jantz, 2011; Freidline *et al.*, 2012; Singh *et al.*, 2012; von Cramon-Taubadel and Smith, 2012), there is another useful method to quantify the magnitude and direction of strain at an arbitrary point of a 3D form in the change from the form to another corresponding form. This method is the finite element scaling method (FESM). This was developed by Lewis *et al.* (1980), Cheverud *et al.* (1983), and their colleagues in the 1980s and has been used by several researchers (Cheverud and Richtsmeier, 1986; Richtsmeier, 1987; Mine and Ogata, 1989; Cheverud *et al.*, 1992; Kohn *et al.*, 1993, 1995; Richtsmeier and Walker, 1993; Mizoguchi, 2000a, b, 2005; Matsukawa, 2002). Both methods are useful for the analysis of form and have many similar strong points. However, one of the major differences between them is that, in generalized Procrustes analysis (GPA), original configurations are standardized by the centroid size, while in finite element scaling analysis (FESA), size is not removed.

In the present study, using the FESM, it is examined whether or not there are any associations between 3D structural deviations in the neighborhood of some cranial landmarks and the degree of occlusal wear on the maxillary first molar (UM1) or age, in order to explore the possibility that masticatory force and/or aging are causes of part of the morphological variation in the human skull.

Materials and Methods

Three male adult samples were used. One consists of 37 skulls of Japanese from the end of the early modern "Edo" period (A.D. 1603 to 1867). These are stored in the University Museum, the University of Tokyo, Japan. The second sample is composed of 30 skulls of African-Americans randomly extracted from the Terry Collection housed in the National Museum of Natural History, Smithsonian Institution, Washington, D.C., U.S.A. They died during the period of 1926 to 1944, and the age-at-death ranges from 21 to 68. The final one is a sample of 35 Indian skulls, which are stored in Nihon University School of Dentistry at Matsudo, Chiba, Japan.

Age-at-death is known for individual specimens of the Terry Collection. For the other two samples, however, there are no such records. Therefore, the degree of occlusal wear on the UM1 was recorded as an indicator of age according to Broca's grading system (Martin and Saller, 1957). It is to be regretted, however, that the present author did not record the degree of dental wear for the sample from the Terry Collection because he did not intend to analyze the relationship between occlusal force and age at that time. Erasing the effect of aging from dental wear is a future task.

All 3D coordinates for cranial landmarks were obtained by the present author on the basis of trigonometric measurements using sliding and spreading calipers. The Japanese skulls were measured twice to assess intra-observer errors during the periods of September, 1976, to January, 1977, and September, 1977, to December, 1977; the African-American skulls, in April and May, 1987; and the Indian skulls, between April, 1994, and October, 1996. Basically, the coordinates of a landmark are calculated using the line segments between the landmark and three of the following five landmarks: nasion, bregma, lambda, right asterion, and left asterion. In the present study, the positive direction of the *x*-axis or anterior-posterior axis of the skull points to the anterior side; that of the *y*-axis or medial-lateral axis points to the left; and that of the *z*-axis or superior-inferior axis points to the superior.

The practical objects analyzed by FESM are six elements or hexahedra set in the cranium (Fig. 1). The eight nodes of each hexahedron are as follows.

1) Right element 1 (anterior neurocranium): nasion (n), grabella (g), bregma (b), basion (ba), right frontotemporale (ft), the center of the right frontal tuber (STH), right eurion (eu), and right porion (po)
2) Left element 1 (anterior neurocranium): n, g, b, ba, left ft, left STH, left eu, and left po
3) Right element 2 (posterior neurocranium): b, ba, inion (i), lambda (l), right eu, right po, right asterion (ast), and the center of the right parietal tuber (SCH)
4) Left element 2 (posterior neurocranium): b, ba, i, l, left eu, left po, left ast, and left SCH
5) Right element 3 (orbito-zygomatic region): g, right frontomalare temporale (fmt), right po, opisthion (o), n, right orbitale (or), right zygomaxillare (zm), and ba
6) Left element 3 (orbito-zygomatic region): g, left fmt, left po, o, n, left or, left zm, and ba

The definitions of the above landmarks except for STH and SCH can be found in Martin and Saller (1957). STH was marked with a pencil by viewing from superior and lateral directions, and SCH, from superior and posterior directions. This method may be somewhat subjective.

For each node of the six hexahedra, the magnitude of 3D structural deviation (from the 'mean' cranium in each sample) called 'principal value' and its direction cosines were first estimated by FESM. The details of the FESM and the relevant procedures are described in Lewis *et al.* (1980), Cheverud *et al.* (1983), Cheverud and Richtsmeier (1986), Leigh and Cheverud (1991), Cheverud *et al.* (1992), Malvern (1969), Bathe and Wilson (1976), and Mizoguchi (2000b). In the present study, principal values were linear-

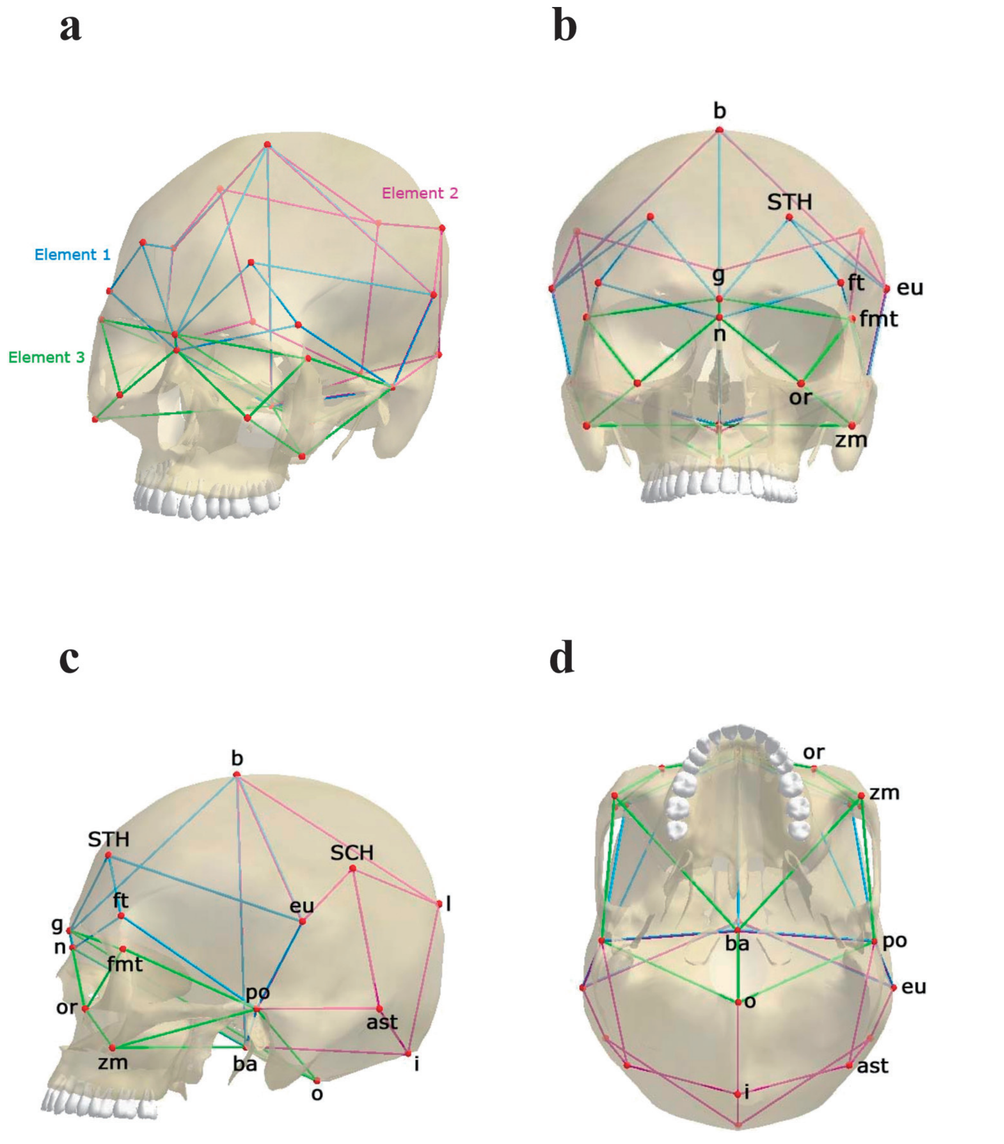

Fig. 1. Elements set up in the cranium and the cranial landmarks used. **a.** Bird's-eye view. **b.** Anterior view. **c.** Lateral view. **d.** Inferior view.

ized using the following formula (Cheverud and Richtsmeier, 1986; Cheverud *et al.*, 1992) before use in multivariate analyses:

$$L_{\mathrm{i}} = \ln\left[(1 + 2P_i)^{1/2}\right],$$

where P_i is the i-th principal value ($i = 1$, 2, and 3), and L_i is the value transformed to a linear or additive scale.

The intra-observer errors for linearized principal values and direction cosines were evaluated by the double determination method (Lundström, 1948; Mizoguchi, 1977). To check the relative magnitude of errors, intraclass correlation coefficients (Cavalli-Sforza and Bodmer, 1971) were calculated between the duplicate data sets of the early modern Japanese sample.

To examine the overall or local relationships between 3D structural strains and dental wear or age, principal component analysis, often abbreviated to PCA, (Lawley and Maxwell, 1963;

Okuno *et al.*, 1971, 1976; Takeuchi and Yanai, 1972) was applied to the correlation matrices. The correlations between age and the principal values and direction cosines were estimated using Pearson's product-moment correlation coefficient, and those between such 3D variables and the degree of occlusal wear on the UM1 were estimated using four-fold point correlation coefficient (Yasuda, 1969).

At this step, however, only six nodes were selected for a set of three elements on one side because of the statistical limitation on the number of variables and sample size. In practice, one set of six nodes was chosen from the viewpoint of a possible relationship with the degree of development of skeletal muscles or growth: ft, STH, i, SCH, g, and zm; and the other set mainly contains intersections of sutures: b, ba, l, ast, fmt, and n.

The number of principal components was determined so that the cumulative proportion of the variances of the principal components exceeded 80%. The principal components obtained were then transformed by Kaiser's normal varimax rotation method (Asano, 1971; Okuno *et al.*, 1971) into different factors in an attempt to reveal other associations behind the variables.

The significance of factor loadings was tested by the bootstrap method (Efron, 1979a, b, 1982; Diaconis and Efron, 1983; Mizoguchi, 1993). In order to estimate the bootstrap standard deviation of a factor loading, 1,000 bootstrap replications, including the observed sample, were used. The bootstrap standard deviation was estimated by directly counting the cumulative frequency for the standard deviation in the bootstrap distribution.

The presence of common factors, such as those represented by principal components (PCs) or rotated factors (Facs), was further tested by evaluating the similarities between the factors obtained for the three samples, namely, by estimating Kendall's rank correlation coefficient, tau (Siegel, 1956), between the patterns of variation of factor loadings. It should be noted here that a certain common factor (PC in practice) extracted from the PCA for a certain sample can be detected as a rotated factor in the rotated solution of the PCs extracted from another similar sample, as shown in Mizoguchi (2004). Therefore, PCs and Facs are equivalently treated in this study.

Mathematical and statistical calculations were executed using programs written by the author in FORTRAN: THRCR3 for calculating 3D coordinates of cranial landmarks, FESM for finite element scaling analysis, MIVCRL for intraclass correlation coefficients, BTPCA for principal component analysis and Kaiser's normal varimax rotation, and RKCNCT for rank correlation coefficients. The FORTRAN 77 compiler used is FTN77 for personal computers, provided by Salford Software Ltd. To increase efficiency during programming and calculation, a GUI for programming, CPad, provided by "kito," was used. 3D illustrations of the human skull were drawn by the present author with Rokkaku-Daiou Super 6 (Ver. 6.3.1) of CELSYS, Inc., utilizing a free 3D model, "Skull N070211–3D model," created by Fahim Fazli as a template.

Results

Intraclass correlations between the duplicate data sets from the early modern Japanese sample are shown in Table 1. The intraclass correlation coefficients independently obtained from the right and left sides reveal at least two similar tendencies. One is that the intra-observer errors on the principal values tend to be lower than those on the corresponding direction cosines in most of the landmarks examined. The other is that, against our expectation, while the intraclass correlation coefficients on the nasion and glabella are extremely low, those on the inion and SCH are relatively high. Such a difference may be partly caused by the use of different sets of three landmarks on which the determination of the coordinates of landmarks in question is based. In any case, the results of the following analyses, especially on the nasion and glabella, must be carefully interpreted.

In Tables 2 to 13, the factor loadings on PCs

Table 1. Intraclass correlation coefficients between the first and second data sets from early modern Japanese in the linearized first principal values and their direction cosines at the eight nodes and centroid of each of six regional elements (hexahedra) of the skull.[1]

Variable[2]	Right	Left
Element 1 (Anterior neurocranium)		
Node 1 (n): 1st p.v.	0.17	0.23
a–p	0.40**	0.64***
m–l	0.05	0.13
s–i	0.68***	0.32*
Node 2 (g): 1st p.v.	0.17	0.20
a–p	0.47**	0.35*
m–l	−0.10[3]	0.56***
s–i	0.37*	0.40**
Node 3 (b): 1st p.v.	0.91***	0.90***
a–p	0.28*	0.66***
m–l	0.41**	0.28*
s–i	0.52***	0.68***
Node 4 (ba): 1st p.v.	0.75***	0.78***
a–p	0.72***	0.84***
m–l	0.71***	0.39**
s–i	0.68***	0.71***
Node 5 (ft): 1st p.v.	0.80***	0.82***
a–p	0.43**	0.61***
m–l	0.43**	0.57***
s–i	0.62***	0.50***
Node 6 (STH): 1st p.v.	0.55***	0.63***
a–p	0.43**	0.34*
m–l	0.45**	0.28*
s–i	0.07	0.46**
Node 7 (eu): 1st p.v.	0.91***	0.89***
a–p	0.73***	0.47**
m–l	0.55***	0.36*
s–i	0.61***	0.56***
Node 8 (po): 1st p.v.	0.88***	0.86***
a–p	0.53***	0.90***
m–l	0.64***	0.83***
s–i	0.41**	0.85***
Centroid: 1st p.v.	0.95***	0.94***
a–p	0.66***	0.51***
m–l	0.68***	0.37*
s–i	0.71***	0.63***
Element 2 (Posterior neurocranium)		
Node 1 (b): 1st p.v.	0.95***	0.93***
a–p	0.71***	0.73***
m–l	0.68***	0.36*
s–i	0.62***	0.41**
Node 2 (ba): 1st p.v.	0.68***	0.85***
a–p	0.68***	0.37*
m–l	0.43**	0.39**
s–i	0.60***	0.71***
Node 3 (i): 1st p.v.	0.97***	0.92***
a–p	0.89***	0.60***
m–l	0.81***	0.67***
s–i	0.97***	0.92***
Node 4 (l): 1st p.v.	0.95***	0.96***
a–p	0.75***	0.74***
m–l	0.86***	0.61***
s–i	0.73***	0.55***
Node 5 (eu): 1st p.v.	0.65***	0.80***
a–p	0.58***	0.79***
m–l	0.33*	0.36*
s–i	0.36*	0.59***
Element 2 (Posterior neurocranium)		
Node 6 (po): 1st p.v.	0.85***	0.81***
a–p	0.65***	0.58***
m–l	0.83***	0.51***
s–i	0.70***	0.59***
Node 7 (ast): 1st p.v.	0.83***	0.63***
a–p	0.86***	0.52***
m–l	0.54***	0.62***
s–i	0.70***	0.71***
Node 8 (SCH): 1st p.v.	0.85***	0.89***
a–p	0.54***	0.76***
m–l	0.42**	0.53***
s–i	0.45**	0.50***
Centroid: 1st p.v.	0.87***	0.90***
a–p	0.85***	0.68***
m–l	0.86***	0.47**
s-i	0.85***	0.68***
Element 3 (Orbito-zygomatic region)		
Node 1 (g): 1st p.v.	0.25	0.26
a–p	0.43**	0.51***
m–l	0.34*	0.00
s–i	0.68***	0.44**
Node 2 (fmt): 1st p.v.	0.59***	0.46**
a–p	0.22	0.51***
m–l	0.37*	0.58***
s–i	0.53***	0.53***
Node 3 (po): 1st p.v.	0.76***	0.76***
a–p	0.72***	0.60***
m–l	0.70***	0.19
s–i	0.75***	0.27
Node 4 (o): 1st p.v.	0.79***	0.84***
a–p	0.61***	0.43**
m–l	0.19	0.23
s–i	0.68***	0.58***
Node 5 (n): 1st p.v.	0.30*	0.09
a–p	0.64***	0.14
m–l	0.34*	0.02
s–i	0.55***	0.47**
Node 6 (or): 1st p.v.	0.66***	0.74***
a–p	0.78***	0.42**
m–l	0.66***	0.43**
s–i	0.55***	0.21
Node 7 (zm): 1st p.v.	0.79***	0.76***
a–p	0.31*	0.45**
m–l	0.40**	0.62***
s–i	0.72***	0.49**
Node 8 (ba): 1st p.v.	0.82***	0.69***
a–p	0.45**	0.57***
m–l	0.47**	0.56***
s–i	0.42**	0.70***
Centroid: 1st p.v.	0.67***	0.80***
a–p	0.81***	0.75***
m–l	0.68***	0.46**
s–i	0.75***	0.57***

[1] The sample size (i.e., no. of pairs) is 32.
[2] p.v.: principal value; a–p: direction cosine for the anterior-posterior axis; m–l: direction cosine for the medial-lateral axis; s–i: direction cosine for the superior-inferior axis.
[3] Underestimate due to a sampling error.
* $P<0.05$; ** $P<0.01$; *** $P<0.001$, by a one-tailed test.

and rotated factors for ft, STH, i, SCH, g, and zm are listed, and, in Tables 14 to 25, those for b, ba, l, ast, fmt, and n are shown. Remarkable findings are as follows.

First, both PC IV from the right elements (Table 2) and PC VIII from the left elements (Table 4) of early modern Japanese have highly significant correlations ($P<0.001$) with the degree of dental wear and the first principal value at the inion (Fig. 2). Furthermore, both PC VIIIs from the right and left elements (Tables 2 and 4) have highly significant positive correlations ($P<0.001$) with dental wear and inverse correlations ($P<0.01$) with the first principal value at the frontotemporale.

Not only Fac II from the right elements (Table 11) but also Fac IX from the left elements (Table 13) of African-Americans reveals that age is significantly associated with the principal value at SCH ($P<0.01$). This association is confirmed by the significant rank correlation coefficient of 0.53 ($P<0.001$) between these factors in the pattern of variation of factor loadings (Table 26).

Both PC IV from the right elements (Table 14) and PC VIII from the left elements (Table 16) of early modern Japanese show that the degree of dental wear is positively associated with the principal value at the frontomalare temporale ($P<0.01$) and inversely associated with the principal value at the asterion ($P<0.001$).

In the data set of Indians, however, no consistent tendency was found with respect to the associations between dental wear and 3D structural deviations at landmarks.

Discussion

To date, several FESAs of the human skull have been conducted. For example, Cheverud *et al.* (1992) and Kohn *et al.* (1993, 1995) examined the effect of artificial cranial vault deformation on the cranial base and face using Native American samples; Richtsmeier (1987) studied morphological differences between the craniofacial complex of normal individuals and those affected with the syndromes of Apert and Crouzon; and Richtsmeier and Walker (1993) extracted properties of the facial skeleton of a juvenile *Homo erectus* from Nariokotome, Kenya, by comparison with the faces of some modern humans, chimpanzees, and simulated *Homo erectus* individuals. To the best of the present author's knowledge, however, there have been no FESAs on the associations of cranial landmarks with dental wear, except for those by Mizoguchi (2000a, 2005).

Associations with dental wear or age

Mizoguchi (2000a), using the same sample from early modern Japanese as used here, carried out FESAs of three neurocranial elements, which were however different from those examined in the present study, and showed that the local shape differences (the so-called standard deviation of transformed principal value) at left frontomalare temporale and left orbitale were inversely correlated with the degree of occlusal wear on the UM1. This implies that those individuals who have weaker dental wear tend to have a more distorted face in the regions near the temporalis muscle.

Furthermore, Mizoguchi (2005), using the same sample and the same neurocranial elements as in his previous work (2000a), revealed that the neurocranium of a person having heavily worn molars tended to be flatter and broader in its anterior-superior part (left STH and right and left ft) and narrower and higher in its posterior-inferior part (right ast and right and left po). He considered that this result suggests that the neurocranial form may partly be determined or modified by the development of the masticatory muscles that produce dental wear. It should be noted in his analyses, however, that, while dental wear was associated with the direction of 3D deviations, it was not so strongly related with their magnitude.

In the present study, a different set of elements from that used by Mizoguchi (2000a, 2005) was examined. Although Mizoguchi (2000a, 2005) dealt with only a limited part of the face, the present study was conducted on a slightly

Table 2. Principal component analysis of the correlations between the linearized first principal values and their direction cosines at six craniofacial landmarks, i.e., ft, STH, i, SCH, g, and zm in the three right elements, and the degree of occlusal wear on the maxillary first molar in early modern Japanese.[1]

Variable[2]	Factor loadings											Total variance (%)
	PC I	II	III	IV	V	VI	VII	VIII	IX	X	XI	
Node 5 (ft) of Element 1: 1st p.v.	0.10	0.48***	0.50***	−0.01	0.32***	0.02	0.26***	−0.15***	0.04	0.15***	0.25***	77.25
a–p	−0.54***	−0.00	0.03	−0.55	0.30	−0.16	−0.32	−0.19	−0.01	−0.10	−0.10	87.79
m–l	−0.03	−0.04	0.06	0.34	−0.33	−0.39	0.57*	0.20	0.28	−0.20	0.11	87.94
s–i	0.55***	−0.08	−0.56	0.29	−0.08	0.30	0.11	0.01	−0.18	0.13	0.14	87.80
Node 6 (STH) of Element 1: 1st p.v.	0.64**	0.01	0.39***	0.27***	0.21***	−0.22***	−0.04	0.18***	−0.04	0.17***	0.20***	83.14
a–p	0.56***	−0.51	−0.35	−0.01	0.03	−0.03	−0.18	−0.05	0.04	−0.16	−0.13	77.10
m–l	−0.56***	0.16	−0.26	0.21	0.09	−0.37	0.09	0.43*	−0.25	0.02	0.03	85.23
s–i	−0.06	0.44	0.24	−0.22	−0.21	0.43	0.44	−0.06	0.18	0.23	−0.29*	90.02
Node 3 (i) of Element 2: 1st p.v.	−0.46*	−0.46***	0.19**	−0.21***	0.13**	0.14***	0.19***	−0.20***	0.29***	0.18***	0.12***	74.22
a–p	0.63***	−0.02	−0.03	−0.18	0.39	0.35	0.27	0.07	−0.12	−0.22	−0.04	84.65
m–l	0.10	0.34	0.06	0.46	0.15	−0.22	−0.47	−0.16	0.23	0.24	0.00	76.14
s–i	−0.64***	−0.25	−0.13	−0.20	−0.36	0.05	−0.08	−0.05	0.19	0.07	0.40***	88.07
Node 8 (SCH) of Element 2: 1st p.v.	0.19	−0.13	0.03	0.03	0.69***	−0.48**	0.18	−0.16	0.10	−0.05	−0.04	83.34
a–p	−0.62***	0.35	−0.40	0.40	0.10	0.17	0.11	0.05	−0.01	0.07	−0.01	88.57
m–l	−0.28	−0.10	−0.17	0.57*	0.24	0.30	−0.23	0.02	0.24	0.07	0.11	71.87
s–i	0.52***	−0.33	0.45	−0.18	−0.28	−0.28	0.02	0.04	0.05	0.08	0.19	81.84
Node 1 (g) of Element 3: 1st p.v.	−0.33	0.64***	0.09	−0.15	−0.11	−0.22**	−0.15*	0.04	−0.07	−0.33***	−0.01	74.66
a–p	−0.08	−0.82***	−0.13	0.13	0.00	−0.08	0.02	−0.17	0.00	0.08	−0.12	77.93
m–l	−0.06	−0.05	0.51	0.12	0.25	0.21	−0.23	0.48*	0.32	−0.00	−0.28*	85.88
s–i	0.38*	0.62	−0.30	−0.14	0.11	−0.06	−0.05	−0.32*	−0.07	0.20	0.14	81.45
Node 7 (zm) of Element 3: 1st p.v.	−0.22	−0.14***	0.38***	0.19***	0.32***	0.49***	−0.07	−0.02	−0.15***	−0.42***	0.37***	93.41
a–p	0.33*	0.31	−0.48	−0.31	0.03	−0.02	−0.05	0.07	0.50**	−0.26	0.24*	92.08
m–l	−0.62***	−0.23	0.09	−0.02	0.35	−0.15	0.27	−0.08	−0.24	0.12	0.07	74.32
s–i	0.07	0.07	0.56	0.28	−0.52	0.03	−0.26	−0.21	−0.20	−0.09	0.03	84.35
Occlusal wear of UM1	0.09	−0.08	−0.07	−0.57***	0.07	0.10	−0.21	0.53***	−0.14	0.34*	0.21	85.66
Total contribution (%)	17.03	12.09	9.95	8.46	7.77	6.54	5.79	4.51	3.89	3.59	3.36	82.99
Cumulative proportion (%)	17.03	29.12	39.07	47.53	55.30	61.85	67.64	72.15	76.04	79.63	82.99	82.99

[1] The sample size is 33. The number of principal components shown here was determined so that the cumulative proportion of the variances of the principal components exceeded 80%.

[2] p.v.: principal value; a–p: direction cosine for the anterior-posterior axis; m–l: direction cosine for the medial-lateral axis; s–i: direction cosine for the superior-inferior axis.

$^{*}P<0.05$; $^{**}P<0.01$; $^{***}P<0.001$, by a two-tailed bootstrap test.

Table 3. Rotated solution of the first eleven principal components extracted from the correlations between the linearized first principal values and their direction cosines at six craniofacial landmarks, i.e., ft, STH, i, SCH, g, and zm in the three right elements, and the degree of occlusal wear on the maxillary first molar in early modern Japanese.[1]

Variable[2]	Factor loadings										
	Fac I	II	III	IV	V	VI	VII	VIII	IX	X	XI
Node 5 (ft) of Element 1: 1st p.v.	0.15	0.02	0.78**	0.01	0.25	0.21	−0.15	−0.02	−0.04	−0.05	−0.06
a–p	−0.13	0.01	−0.09	−0.42*	0.18	−0.00	0.08	0.11	−0.00	−0.72***	0.33*
m–l	0.04	−0.01	0.03	0.90***	0.03	−0.10	0.07	−0.20	0.03	0.05	0.04
s–i	−0.10	0.32	−0.19	−0.04	−0.08	−0.00	0.02	0.06	0.18	0.78***	−0.28
Node 6 (STH) of Element 1: 1st p.v.	0.51*	−0.13	0.16	0.15	0.29	0.14	−0.37	0.16	−0.10	0.31	−0.37
a–p	0.30	0.03	−0.63*	−0.16	0.17	−0.07	0.07	−0.08	0.23	0.37**	−0.12
m–l	−0.60*	0.06	−0.11	0.42*	0.10	−0.06	−0.05	0.34*	−0.26	−0.30*	−0.10
s–i	−0.08	−0.19	0.73***	−0.09	−0.28	−0.30	0.33*	−0.19	0.05	0.08	0.07
Node 3 (i) of Element 2: 1st p.v.	0.01	−0.13	0.04	−0.05	0.12	0.08	0.13	−0.03	−0.14	−0.04	0.82***
a–p	0.21	−0.07	0.13	−0.24	0.35	0.24	0.43*	0.01	0.25	0.43**	−0.34
m–l	−0.07	−0.07	0.08	−0.09	0.07	−0.09	−0.82***	−0.14	0.05	−0.03	−0.19
s–i	−0.17	0.18	−0.15	0.15	−0.40	0.08	−0.01	0.19	0.05	−0.24	0.71***
Node 8 (SCH) of Element 2: 1st p.v.	0.11	0.01	−0.04	0.04	0.89***	0.00	−0.11	−0.10	−0.00	−0.04	−0.02
a–p	−0.90***	0.07	0.13	0.13	−0.10	0.03	−0.14	−0.05	−0.06	−0.02	0.06
m–l	−0.49**	−0.24	−0.15	−0.02	−0.03	0.29	−0.43	−0.11	0.02	0.27	0.21
s–i	0.86***	−0.01	−0.04	0.20	−0.02	−0.05	−0.02	0.11	−0.05	0.10	0.03
Node 1 (g) of Element 3: 1st p.v.	−0.20	0.10	0.24	0.09	−0.17	0.03	−0.03	−0.03	0.13	−0.70***	−0.29
a–p	0.10	−0.02	−0.60	−0.00	0.15	−0.06	0.06	−0.14	−0.30	0.26	0.44**
m–l	0.05	−0.89***	0.10	−0.04	0.02	0.13	−0.13	0.09	−0.06	−0.07	−0.03
s–i	−0.02	0.50*	0.37	−0.28	0.11	−0.20	−0.22	0.02	0.35*	0.07	−0.34*
Node 7 (zm) of Element 3: 1st p.v.	−0.07	−0.18	0.08	−0.11	−0.03	0.92***	0.07	−0.08	−0.12	−0.01	0.12
a–p	−0.01	0.13	−0.00	0.04	0.09	−0.08	0.01	0.10	0.93***	−0.01	−0.09
m–l	−0.31	0.09	0.04	0.07	0.34	0.14	0.13	0.10	−0.50**	−0.22	0.41**
s–i	0.41**	0.00	0.09	0.06	−0.55**	0.19	−0.25	−0.31	−0.35*	−0.13	−0.18
Occlusal wear of UM1	0.15	−0.09	−0.00	−0.23	−0.06	−0.08	0.15	0.85***	0.10	0.00	0.04

[1] The sample size is 33. The cumulative proportion of the variances of the eleven principal components is 82.99%.
[2] p.v.: principal value; a–p: direction cosine for the anterior-posterior axis; m–l: direction cosine for the medial-lateral axis; s–i: direction cosine for the superior-inferior axis.
* $P<0.05$; ** $P<0.01$; *** $P<0.001$, by a two-tailed bootstrap test.

Table 4. Principal component analysis of the correlations between the linearized first principal values and their direction cosines at six craniofacial landmarks, i.e., ft, STH, i, SCH, g, and zm in the three left elements, and the degree of occlusal wear on the maxillary first molar in early modern Japanese.[1]

Variable[2]	Factor loadings										Total variance (%)
	PC I	II	III	IV	V	VI	VII	VIII	IX	X	
Node 5 (ft) of Element 1: 1st p.v.	−0.32	0.15	0.56***	−0.36***	0.42***	0.14*	0.08	−0.18**	0.09	0.06	81.59
a–p	0.56***	−0.05	0.53	−0.05	−0.08	−0.34	0.11	0.27	0.30*	−0.03	90.26
m–l	0.67***	−0.02	−0.45	−0.14	−0.03	0.23	−0.23	−0.12	0.18	0.12	83.69
s–i	−0.61***	−0.06	−0.07	0.29	−0.18	−0.08	0.09	−0.00	−0.29	0.38*	73.71
Node 6 (STH) of Element 1: 1st p.v.	−0.18	0.62***	0.21*	−0.14	0.48***	0.16*	0.39***	−0.01	−0.15	−0.07	91.31
a–p	0.43**	0.15	−0.08	−0.07	−0.00	−0.23	0.52*	0.48*	−0.07	−0.11	78.61
m–l	0.73***	−0.11	−0.26	−0.14	0.10	0.12	−0.29	−0.18	−0.05	0.20	81.78
s–i	−0.61***	−0.15	0.26	0.34	−0.26	0.01	−0.14	−0.00	0.22	0.29	79.47
Node 3 (i) of Element 2: 1st p.v.	0.24	−0.30***	0.27***	0.59***	0.26***	0.18***	−0.11**	0.16***	−0.02	−0.18***	73.71
a–p	0.02	0.27	−0.11	−0.09	−0.47	0.35	0.58**	0.05	0.12	0.11	80.39
m–l	−0.51***	−0.04	−0.07	−0.04	0.31	−0.26	−0.34	0.46*	−0.12	−0.04	78.49
s–i	0.29	−0.49	0.42	0.48	−0.30	−0.07	−0.09	−0.20	0.05	−0.04	86.15
Node 8 (SCH) of Element 2: 1st p.v.	0.15	0.54***	0.39*	0.29	0.05	0.25	−0.33**	0.31**	0.00	−0.10	83.57
a–p	−0.29*	−0.26	0.02	−0.09	−0.06	0.80***	0.04	0.13	0.26	−0.04	89.25
m–l	−0.29	−0.45	−0.51	−0.19	−0.12	−0.44	0.11	0.01	−0.01	−0.05	80.61
s–i	0.38**	0.32	0.46	−0.03	0.05	−0.39*	0.07	−0.20	−0.24	0.44**	91.66
Node 1 (g) of Element 3: 1st p.v.	−0.06	−0.31***	0.43***	−0.50***	0.00	−0.02	−0.25**	0.15	−0.21**	−0.05	67.07
a–p	0.07	−0.03	−0.15	0.68*	0.23	−0.09	0.41	−0.31	−0.03	−0.19	85.42
m–l	0.00	0.40	−0.28	−0.12	0.40	−0.09	−0.10	0.04	0.52**	0.34*	82.32
s–i	0.17	−0.13	0.34	−0.42	−0.57	0.21	0.08	0.13	−0.26*	0.08	80.49
Node 7 (zm) of Element 3: 1st p.v.	0.04	0.61***	0.10	0.50***	−0.27***	−0.01	−0.13*	0.10*	0.05	0.15***	76.49
a–p	−0.01	−0.61**	0.40	−0.18	0.22	−0.18	0.21	−0.15	0.38*	0.01	84.80
m–l	0.31	−0.33	−0.18	0.11	0.39	0.32	0.02	0.15	−0.51**	0.19	82.27
s–i	−0.06	0.64**	−0.13	−0.16	−0.38	−0.22	−0.29	−0.10	0.02	−0.34*	85.68
Occlusal wear of UM1	0.10	−0.23	−0.18	0.17	−0.01	−0.07	0.10	0.71***	0.18	0.19	70.47
Total contribution (%)	12.99	12.44	10.16	9.51	7.91	7.29	6.42	6.06	5.11	3.70	81.57
Cumulative proportion (%)	12.99	25.42	35.59	45.10	53.01	60.29	66.71	72.77	77.87	81.57	81.57

[1] The sample size is 33. The number of principal components shown here was determined so that the cumulative proportion of the variances of the principal components exceeded 80%.

[2] p.v.: principal value; a–p: direction cosine for the anterior-posterior axis; m–l: direction cosine for the medial-lateral axis; s–i: direction cosine for the superior-inferior axis.

* $P<0.05$; ** $P<0.01$; *** $P<0.001$, by a two-tailed bootstrap test.

Table 5. Rotated solution of the first ten principal components extracted from the correlations between the linearized first principal values and their direction cosines at six craniofacial landmarks, i.e., ft, STH, i, SCH, g, and zm in the three left elements, and the degree of occlusal wear on the maxillary first molar in early modern Japanese.[1]

Variable[2]	Factor loadings									
	Fac I	II	III	IV	V	VI	VII	VIII	IX	X
Node 5 (ft) of Element 1: 1st p.v.	−0.15	−0.01	0.12	−0.25	0.67*	−0.01	−0.05	−0.31	0.38	0.13
a–p	0.23	0.17	0.28	−0.16	−0.12	−0.35	0.05	0.46	0.60**	−0.06
m–l	0.72***	−0.14	0.01	−0.01	−0.39*	0.04	0.20	−0.05	−0.13	0.30*
s–i	−0.76*	−0.17	−0.17	0.06	−0.06	−0.07	0.03	−0.11	−0.28	−0.02
Node 6 (STH) of Element 1: 1st p.v.	−0.03	−0.00	0.22	0.12	0.90***	−0.09	0.08	0.03	−0.13	0.10
a–p	0.24	−0.00	−0.04	0.07	0.16	−0.20	0.17	0.78***	−0.03	−0.09
m–l	0.71***	−0.31	0.02	−0.08	−0.34*	−0.20	0.06	−0.14	−0.06	0.17
s–i	−0.78**	0.07	0.12	−0.03	−0.25	0.15	−0.00	−0.22	0.16	0.10
Node 3 (i) of Element 2: 1st p.v.	0.03	−0.36	0.45	0.33	−0.19	0.14	−0.26	0.08	0.29	−0.28
a–p	−0.09	0.12	−0.01	−0.01	0.12	0.17	0.81***	0.22	−0.17	0.01
m–l	−0.35	0.00	−0.09	−0.18	0.11	0.13	−0.71***	0.17	−0.18	0.14
s–i	−0.08	−0.10	0.22	0.15	−0.55*	−0.14	0.07	−0.13	0.49**	−0.44*
Node 8 (SCH) of Element 2: 1st p.v.	0.03	0.10	0.88***	−0.06	0.10	−0.00	−0.13	0.08	−0.14	0.00
a–p	−0.12	−0.22	0.12	−0.20	0.06	0.82***	0.27	−0.15	0.12	0.04
m–l	−0.14	0.10	−0.81***	0.03	−0.23	0.07	−0.19	0.15	−0.06	0.00
s–i	0.03	−0.07	0.23	−0.11	0.13	−0.89***	0.13	−0.04	0.13	0.04
Node 1 (g) of Element 3: 1st p.v.	0.02	−0.07	−0.06	−0.67*	0.10	−0.02	−0.26	−0.06	0.24	−0.26
a–p	−0.05	−0.14	−0.01	0.89***	0.02	−0.08	0.06	0.00	0.07	−0.19
m–l	0.13	0.10	0.05	0.11	0.15	−0.03	−0.08	0.04	−0.01	0.87***
s–i	0.02	−0.01	0.02	−0.67**	−0.08	−0.06	0.44*	0.07	0.02	−0.39*
Node 7 (zm) of Element 3: 1st p.v.	−0.24	0.24	0.62*	0.21	−0.15	−0.22	0.15	0.07	−0.32	0.13
a–p	−0.04	−0.09	−0.28	−0.06	0.03	0.03	−0.06	−0.04	0.86***	−0.01
m–l	0.24	−0.84**	−0.01	0.03	−0.00	0.02	−0.11	0.07	−0.17	−0.14
s–i	0.13	0.76***	0.13	−0.09	0.02	−0.12	−0.03	−0.10	−0.46**	−0.01
Occlusal wear of UM1	−0.13	−0.23	0.02	−0.04	−0.29	0.17	−0.09	0.68**	0.04	0.21

[1] The sample size is 33. The cumulative proportion of the variances of the ten principal components is 81.57%.
[2] p.v.: principal value; a–p: direction cosine for the anterior-posterior axis; m–l: direction cosine for the medial-lateral axis; s–i: direction cosine for the superior-inferior axis.
* $P<0.05$; ** $P<0.01$; *** $P<0.001$, by a two-tailed bootstrap test.

Table 6. Principal component analysis of the correlations between the linearized first principal values and their direction cosines at six craniofacial landmarks, i.e., ft, STH, i, SCH, g, and zm in the three right elements, and the degree of occlusal wear on the maxillary first molar in Indians.[1]

Variable[2]	Factor loadings										Total variance (%)
	PC I	II	III	IV	V	VI	VII	VIII	IX	X	
Node 5 (ft) of Element 1: 1st p.v.	0.52	−0.45	−0.10	−0.29	−0.45	0.10	−0.08	0.10	−0.06	0.16	83.08
a–p	−0.35	−0.12	0.71	0.08	0.26	0.12	−0.07	0.10	−0.30	0.06	83.60
m–l	0.38	0.49	−0.18	0.15	−0.20	−0.46	0.05	−0.26	0.26	−0.08	82.43
s–i	0.18	−0.33	−0.60	0.11	−0.09	0.01	−0.08	−0.27	−0.06	−0.46*	81.82
Node 6 (STH) of Element 1: 1st p.v.	0.34	−0.13	−0.68	−0.27	−0.03	0.17	−0.21	0.15	−0.08	0.23	82.16
a–p	−0.57	0.22	0.04	−0.33	0.55	−0.07	−0.10	−0.15	0.13	−0.18	86.67
m–l	0.42	0.11	0.41	0.17	−0.20	−0.20	0.54*	−0.18	−0.23	0.01	84.28
s–i	0.46	−0.40	−0.03	0.25	−0.35	0.03	−0.36	0.14	0.23	−0.01	76.40
Node 3 (i) of Element 2: 1st p.v.	0.17	−0.62	0.09	−0.08	0.13	0.22	0.38	−0.21	0.13	−0.08	71.03
a–p	−0.77	−0.02	0.02	−0.10	−0.31	−0.25	−0.10	0.05	0.23	−0.03	82.53
m–l	0.45	0.36	0.51	0.16	−0.19	0.07	−0.38	0.07	−0.26	0.04	87.42
s–i	0.38	−0.48	0.02	−0.01	0.33	0.41	0.33	−0.23	0.03	0.20	85.66
Node 8 (SCH) of Element 2: 1st p.v.	0.26	−0.15	0.25	−0.51	0.06	0.02	−0.14	0.43	0.36	−0.29	83.74
a–p	−0.30	−0.41	0.43	−0.44	−0.36	−0.11	−0.00	−0.32	0.08	−0.01	89.01
m–l	−0.41	0.09	−0.30	−0.37	0.04	0.47	−0.18	−0.34	0.08	0.30	86.62
s–i	0.04	0.44	−0.60	0.28	0.39	−0.05	0.17	0.20	−0.12	0.08	87.27
Node 1 (g) of Element 3: 1st p.v.	0.01	−0.45	0.04	0.33	0.50	−0.22	−0.34	0.08	−0.07	0.15	76.05
a–p	0.16	0.67	−0.14	−0.54	−0.14	−0.01	−0.07	−0.15	−0.10	0.23	89.37
m–l	−0.39	0.09	−0.12	0.27	−0.26	0.48	0.35	0.40	0.09	−0.18	86.82
s–i	−0.09	−0.50	−0.18	0.44	0.23	−0.33	−0.25	−0.24	0.12	0.09	79.36
Node 7 (zm) of Element 3: 1st p.v.	0.15	−0.19	0.16	−0.24	0.19	−0.53	0.29	0.28	0.28	0.43	89.18
a–p	−0.27	0.13	0.22	0.57	−0.17	0.42	−0.08	0.02	0.39	0.29	90.73
m–l	0.48	0.10	0.40	−0.19	0.43	0.23	−0.29	−0.05	−0.07	−0.19	79.30
s–i	−0.30	−0.47	−0.31	−0.31	0.09	−0.14	0.14	0.31	−0.32	−0.04	74.77
Occlusal wear of UM1	−0.54	−0.35	−0.03	0.10	−0.44	−0.14	−0.11	−0.02	−0.42*	0.09	84.06
Total contribution (%)	14.38	12.99	11.61	9.17	8.68	7.02	6.00	4.91	4.56	4.00	83.34
Cumulative proportion (%)	14.38	27.38	38.99	48.15	56.84	63.86	69.86	74.77	79.33	83.34	83.34

[1] The sample size is 35. The number of principal components shown here was determined so that the cumulative proportion of the variances of the principal components exceeded 80%.

[2] p.v.: principal value; a–p: direction cosine for the anterior-posterior axis; m–l: direction cosine for the medial-lateral axis; s–i: direction cosine for the superior-inferior axis.

* $P<0.05$; ** $P<0.01$; *** $P<0.001$, by a two-tailed bootstrap test.

Table 7. Rotated solution of the first ten principal components extracted from the correlations between the linearized first principal values and their direction cosines at six craniofacial landmarks, i.e., ft, STH, i, SCH, g, and zm in the three right elements, and the degree of occlusal wear on the maxillary first molar in Indians.[1]

Variable[2]	Factor loadings									
	Fac I	II	III	IV	V	VI	VII	VIII	IX	X
Node 5 (ft) of Element 1: 1st p.v.	0.81*	0.04	−0.07	−0.22	−0.10	−0.24	0.20	0.00	0.10	0.05
a–p	−0.36	0.30	0.19	−0.29	0.11	0.17	−0.04	0.66***	−0.08	0.14
m–l	0.03	0.08	0.23	0.14	−0.09	−0.00	−0.22	−0.82***	−0.08	0.03
s–i	0.24	−0.23	−0.06	0.10	0.25	−0.33	0.19	−0.27	0.01	−0.64**
Node 6 (STH) of Element 1: 1st p.v.	0.53	−0.05	−0.52	0.38	−0.02	−0.34	0.07	−0.07	0.05	−0.03
a–p	−0.82*	−0.02	−0.34	−0.07	0.06	−0.13	−0.10	0.06	0.19	0.02
m–l	0.08	0.20	0.70***	−0.09	−0.27	−0.02	0.25	−0.18	−0.31	0.17
s–i	0.72	0.09	0.07	−0.11	0.33	0.18	0.00	−0.12	0.23	−0.13
Node 3 (i) of Element 2: 1st p.v.	0.09	−0.13	0.10	−0.24	0.12	−0.07	0.77***	0.08	0.11	−0.04
a–p	−0.26	−0.56	−0.15	−0.43	0.04	0.13	−0.47*	0.06	0.02	0.04
m–l	0.27	0.75**	0.27	−0.03	−0.15	0.20	−0.32	0.04	−0.05	−0.01
s–i	0.15	0.15	−0.07	0.06	0.10	0.01	0.88***	0.11	−0.04	0.06
Node 8 (SCH) of Element 2: 1st p.v.	0.12	0.14	0.01	−0.18	−0.12	−0.15	0.03	0.07	0.84***	0.16
a–p	−0.02	−0.13	−0.05	−0.92***	−0.06	−0.10	0.07	0.09	−0.00	0.08
m–l	−0.17	−0.08	−0.85***	−0.11	−0.20	0.09	0.09	0.06	−0.19	−0.09
s–i	−0.18	−0.13	−0.07	0.87***	−0.00	−0.08	−0.09	−0.14	−0.16	0.00
Node 1 (g) of Element 3: 1st p.v.	−0.01	0.15	0.00	0.12	0.80***	−0.06	0.05	0.24	−0.00	0.13
a–p	−0.04	0.29	−0.37	0.08	−0.62**	−0.22	−0.27	−0.33	−0.13	0.19
m–l	−0.02	−0.52*	0.10	0.22	−0.35	0.45	−0.01	0.35	0.09	−0.28
s–i	0.02	−0.15	−0.03	−0.04	0.85***	0.00	0.08	−0.12	−0.17	−0.04
Node 7 (zm) of Element 3: 1st p.v.	0.04	−0.15	0.15	−0.03	0.14	−0.18	0.12	−0.10	0.19	0.86***
a–p	0.01	−0.07	−0.08	0.00	0.07	0.93***	−0.04	0.09	−0.12	−0.01
m–l	−0.10	0.79***	0.02	0.02	0.00	−0.08	0.19	0.07	0.34	−0.06
s–i	0.04	−0.46*	−0.10	0.01	0.10	−0.56**	0.04	0.45*	0.05	0.06
Occlusal wear of UM1	0.15	−0.39	−0.01	−0.38	0.15	−0.10	−0.32	0.40	−0.45*	−0.15

[1] The sample size is 35. The cumulative proportion of the variances of the ten principal components is 83.34%.
[2] p.v.: principal value; a–p: direction cosine for the anterior-posterior axis; m–l: direction cosine for the medial-lateral axis; s–i: direction cosine for the superior-inferior axis.
* $P<0.05$; ** $P<0.01$; *** $P<0.001$, by a two-tailed bootstrap test.

Table 8. Principal component analysis of the correlations between the linearized first principal values and their direction cosines at six craniofacial landmarks, i.e., ft, STH, i, SCH, g, and zm in the three left elements, and the degree of occlusal wear on the maxillary first molar in Indians.[1]

Variable[2]	Factor loadings										Total variance (%)
	PC I	II	III	IV	V	VI	VII	VIII	IX	X	
Node 5 (ft) of Element 1: 1st p.v.	−0.21	−0.76	−0.26	−0.07	0.33	0.21	0.09	0.04	−0.18	0.09	90.05
a–p	0.36	0.27	−0.28	0.66	−0.11	0.24	−0.03	0.21	0.07	0.31*	93.97
m–l	0.48	−0.16	0.56	−0.23	−0.02	−0.21	−0.22	0.25	−0.20	−0.03	81.25
s–i	−0.50	0.34	0.29	0.11	−0.03	0.07	0.21	−0.35	0.28	−0.44*	91.60
Node 6 (STH) of Element 1: 1st p.v.	−0.37	−0.31	−0.51	−0.21	0.36	0.03	0.06	−0.02	−0.48*	−0.03	90.79
a–p	0.27	0.73	−0.41	0.21	−0.10	−0.00	0.08	−0.11	0.10	0.03	85.66
m–l	0.42	−0.16	0.50	0.11	−0.04	−0.35	−0.31	−0.06	−0.27	−0.23	81.06
s–i	−0.50	−0.27	0.29	0.33	0.29	0.08	0.18	−0.05	0.29	0.19	74.98
Node 3 (i) of Element 2: 1st p.v.	0.38	−0.35	−0.15	0.11	0.57*	0.15	0.10	−0.02	0.14	−0.32	77.81
a–p	−0.35	0.07	0.46	0.36	−0.02	0.05	0.55*	0.15	−0.27	−0.10	88.13
m–l	−0.53	−0.18	−0.08	−0.32	−0.18	−0.30	−0.19	0.06	0.19	−0.03	61.15
s–i	0.65	−0.01	−0.36	−0.08	0.29	0.18	−0.40	0.07	0.23	−0.13	91.68
Node 8 (SCH) of Element 2: 1st p.v.	−0.32	−0.45	−0.21	0.41	0.12	−0.37	−0.13	−0.24	0.07	0.12	75.16
a–p	0.14	−0.63	0.29	0.08	−0.52	0.38	0.01	−0.14	0.05	−0.08	94.29
m–l	−0.24	−0.14	0.46	0.25	0.43	−0.21	−0.27	−0.09	0.13	0.42*	85.59
s–i	−0.22	0.73	−0.20	−0.18	0.41	−0.18	0.08	0.25	−0.11	−0.01	93.55
Node 1 (g) of Element 3: 1st p.v.	0.57	−0.15	−0.16	0.28	0.05	−0.19	0.44	−0.27	−0.24	0.09	82.50
a–p	−0.49	0.01	−0.31	−0.18	−0.43	0.43	−0.11	0.03	−0.12	0.15	79.34
m–l	−0.42	0.20	0.06	0.49	0.18	−0.12	−0.13	0.58**	−0.01	−0.26	93.08
s–i	0.56	0.16	0.17	−0.32	0.30	−0.00	0.38	−0.28	0.12	0.08	79.85
Node 7 (zm) of Element 3: 1st p.v.	0.10	−0.18	−0.25	0.71	−0.01	0.18	−0.29	−0.19	−0.10	−0.27	83.83
a–p	0.08	−0.43	0.07	−0.24	0.20	0.35	0.20	0.44	0.34	−0.08	77.19
m–l	0.18	−0.33	−0.25	0.03	−0.26	−0.59*	0.21	0.16	0.30	0.08	78.04
s–i	−0.22	0.39	0.39	−0.13	0.35	0.34	−0.34	−0.38	−0.04	0.10	87.21
Occlusal wear of UM1	0.37	0.11	0.45	0.14	−0.00	0.34	0.07	0.32	−0.10	0.21	64.67
Total contribution (%)	15.13	13.57	10.78	9.10	7.87	7.00	5.99	5.67	4.33	3.85	83.30
Cumulative proportion (%)	15.13	28.70	39.49	48.59	56.45	63.46	69.45	75.12	79.45	83.30	83.30

[1] The sample size is 35. The number of principal components shown here was determined so that the cumulative proportion of the variances of the principal components exceeded 80%.

[2] p.v.: principal value; a–p: direction cosine for the anterior-posterior axis; m–l: direction cosine for the medial-lateral axis; s–i: direction cosine for the superior-inferior axis.

* $P<0.05$; ** $P<0.01$; *** $P<0.001$, by a two-tailed bootstrap test.

Table 9. Rotated solution of the first ten principal components extracted from the correlations between the linearized first principal values and their direction cosines at six craniofacial landmarks, i.e., ft, STH, i, SCH, g, and zm in the three left elements, and the degree of occlusal wear on the maxillary first molar in Indians.[1]

Variable[2]	Factor loadings									
	Fac I	II	III	IV	V	VI	VII	VIII	IX	X
Node 5 (ft) of Element 1: 1st p.v.	0.02	−0.28	−0.14	−0.09	0.18	−0.08	0.22	0.02	−0.82***	0.20
a–p	0.16	0.02	−0.22	0.86***	0.03	−0.13	−0.12	0.21	0.21	0.01
m–l	0.07	−0.09	0.86***	0.02	−0.04	−0.02	0.20	−0.11	0.08	−0.03
s–i	−0.50	0.01	−0.34	−0.42	0.18	0.34	−0.12	0.09	0.45	0.03
Node 6 (STH) of Element 1: 1st p.v.	−0.00	0.19	−0.21	−0.21	0.04	0.03	−0.09	0.06	−0.87***	−0.08
a–p	0.17	0.41	−0.35	0.38	0.03	−0.02	−0.34	−0.08	0.42	−0.31
m–l	0.01	−0.18	0.82***	−0.02	0.17	−0.00	−0.24	0.03	0.14	0.03
s–i	−0.37	−0.13	−0.26	−0.07	0.11	0.07	0.18	0.12	−0.05	0.68***
Node 3 (i) of Element 2: 1st p.v.	0.18	−0.06	0.03	0.09	0.79***	−0.03	0.20	−0.09	−0.23	0.04
a–p	−0.91***	0.01	0.04	0.14	0.01	0.05	0.06	0.12	0.01	0.07
m–l	0.07	0.01	−0.11	−0.62***	−0.32	−0.18	0.05	0.22	−0.06	0.13
s–i	0.78***	0.05	0.08	0.23	0.44*	0.03	0.13	−0.02	0.03	−0.18
Node 8 (SCH) of Element 2: 1st p.v.	0.02	−0.16	−0.16	−0.16	0.12	−0.31	−0.39	0.21	−0.27	0.54*
a–p	−0.09	−0.95***	0.09	0.02	−0.04	−0.03	0.14	−0.02	0.00	−0.07
m–l	−0.03	0.06	0.22	0.00	−0.03	0.17	−0.03	0.04	0.01	0.88***
s–i	−0.06	0.93***	−0.13	−0.03	−0.06	0.17	0.01	0.06	0.03	−0.12
Node 1 (g) of Element 3: 1st p.v.	−0.12	−0.09	0.11	0.41	0.35	−0.38	−0.34	−0.47	−0.14	−0.09
a–p	0.04	−0.21	−0.48*	−0.08	−0.56**	0.20	0.04	0.23	−0.21	−0.25
m–l	−0.29	0.36	0.03	0.08	0.10	−0.03	0.09	0.81***	0.07	0.15
s–i	0.04	0.16	0.13	0.09	0.30	0.06	0.14	−0.78***	0.16	−0.06
Node 7 (zm) of Element 3: 1st p.v.	0.12	−0.35	−0.12	0.32	0.42	0.05	−0.45*	0.45*	−0.07	0.02
a–p	0.05	−0.19	−0.04	−0.03	0.23	−0.09	0.81***	−0.00	−0.15	0.01
m–l	0.10	−0.05	0.03	−0.12	−0.00	−0.86***	−0.01	−0.06	0.08	0.07
s–i	0.04	0.14	0.00	−0.08	−0.06	0.86***	−0.07	−0.12	0.13	0.26
Occlusal wear of UM1	−0.14	−0.09	0.33	0.56**	−0.06	0.20	0.35	−0.06	0.17	0.00

[1] The sample size is 35. The cumulative proportion of the variances of the ten principal components is 83.30%.
[2] p.v.: principal value; a–p: direction cosine for the anterior-posterior axis; m–l: direction cosine for the medial-lateral axis; s–i: direction cosine for the superior-inferior axis.
* $P<0.05$; ** $P<0.01$; *** $P<0.001$, by a two-tailed bootstrap test.

Table 10. Principal component analysis of the correlations between the linearized first principal values and their direction cosines at six craniofacial landmarks, i.e., ft, STH, i, SCH, g, and zm in the three right elements, and age in African-Americans.[1]

Variable[2]	Factor loadings									Total variance (%)
	PC I	II	III	IV	V	VI	VII	VIII	IX	
Node 5 (ft) of Element 1: 1st p.v.	−0.34	0.44***	−0.12	0.39***	−0.54***	0.02	0.26**	−0.24**	0.04	89.91
a–p	0.72***	−0.05	0.27	0.09	−0.32	−0.27	0.01	−0.12	0.04	79.47
m–l	−0.32	0.32	−0.34	0.16	0.37	−0.09	−0.53*	−0.01	0.23	82.10
s–i	−0.67***	−0.51	0.10	−0.25	0.01	0.10	0.01	0.14	−0.00	81.15
Node 6 (STH) of Element 1: 1st p.v.	−0.53*	0.41***	−0.23**	0.26***	−0.46***	−0.11	0.25**	−0.11	0.06	86.92
a–p	0.38*	−0.49	0.36	−0.13	−0.24	−0.20	−0.38*	−0.29	0.15	88.23
m–l	0.08	0.19	−0.62	−0.42	0.20	0.12	0.22	−0.25	0.33*	87.18
s–i	−0.52**	0.22	0.25	0.41	−0.09	0.28	0.03	0.30*	−0.21	77.49
Node 3 (i) of Element 2: 1st p.v.	0.36	0.23*	0.31***	−0.04	−0.06	0.47***	−0.07	−0.05	0.64***	92.21
a–p	0.28	−0.06	−0.48	0.13	−0.34	−0.47	−0.05	−0.25	−0.04	73.83
m–l	0.01	−0.00	0.41	−0.69*	−0.08	−0.20	0.04	0.21	−0.06	73.24
s–i	−0.30	−0.06	0.45	0.31	0.15	0.62**	0.00	−0.23	0.05	85.60
Node 8 (SCH) of Element 2: 1st p.v.	−0.11	0.69***	0.11	−0.44**	−0.29*	0.10	−0.17	0.08	0.00	82.43
a–p	0.75***	0.12	−0.20	−0.03	0.01	0.31	0.06	0.08	−0.19	75.80
m–l	0.00	−0.48*	−0.55	0.21	0.30	0.15	0.03	−0.06	0.13	71.21
s–i	−0.74***	0.05	0.20	0.10	0.07	−0.32	0.03	−0.18	0.12	75.67
Node 1 (g) of Element 3: 1st p.v.	−0.42	−0.57***	−0.22	−0.18	−0.31**	0.23**	0.21**	−0.12	0.11	80.30
a–p	0.60**	0.42	0.36	0.33	−0.02	0.08	0.24	0.11	0.10	86.32
m–l	−0.30	0.41	0.08	−0.01	0.66**	−0.39	0.08	−0.09	−0.01	86.50
s–i	−0.19	−0.52	−0.31	−0.25	−0.34	0.34	−0.23	0.01	−0.15	76.78
Node 7 (zm) of Element 3: 1st p.v.	−0.14	−0.36***	0.18*	−0.30***	0.03	−0.27***	0.59***	0.28**	0.34***	88.68
a–p	0.07	0.52	−0.51	−0.40	0.04	0.24	0.07	−0.06	−0.13	77.43
m–l	−0.43**	0.11	0.54	−0.26	−0.06	−0.00	−0.17	−0.47*	−0.04	81.15
s–i	−0.08	−0.29	−0.17	0.55*	−0.19	−0.19	−0.27	0.39*	0.29	80.23
Age	−0.30	0.49*	−0.17	−0.33	−0.36	−0.05	−0.32	0.36	0.20	87.78
Total contribution (%)	17.15	14.02	11.37	9.78	7.95	7.34	5.49	4.73	4.08	81.90
Cumulative proportion (%)	17.15	31.17	42.53	52.31	60.26	67.60	73.10	77.83	81.90	81.90

[1] The sample size is 27. The number of principal components shown here was determined so that the cumulative proportion of the variances of the principal components exceeded 80%.

[2] p.v.: principal value; a–p: direction cosine for the anterior-posterior axis; m–l: direction cosine for the medial-lateral axis; s–i: direction cosine for the superior-inferior axis.

* $P<0.05$; ** $P<0.01$; *** $P<0.001$, by a two-tailed bootstrap test.

Table 11. Rotated solution of the first nine principal components extracted from the correlations between the linearized first principal values and their direction cosines at six craniofacial landmarks, i.e., ft, STH, i, SCH, g, and zm in the three right elements, and age in African-Americans.[1]

Variable[2]	Factor loadings								
	Fac I	II	III	IV	V	VI	VII	VIII	IX
Node 5 (ft) of Element 1: 1st p.v.	0.04	0.10	0.01	0.93***	0.08	0.06	−0.09	0.05	0.04
a–p	0.33	−0.02	0.02	0.01	−0.40	−0.70***	0.12	0.16	−0.04
m–l	0.15	0.14	−0.38	−0.08	0.42	0.24	−0.55*	−0.29	−0.01
s–i	−0.64	−0.01	0.00	−0.16	0.46*	0.24	0.27	0.18	0.02
Node 6 (STH) of Element 1: 1st p.v.	−0.03	0.19	−0.07	0.85***	0.24	0.19	−0.01	−0.03	−0.11
a–p	−0.16	−0.07	0.01	−0.31	0.03	−0.84***	−0.01	0.18	0.10
m–l	−0.06	0.03	0.08	0.04	−0.08	0.11	0.03	−0.92***	0.02
s–i	−0.02	0.09	−0.06	0.31	0.14	0.54*	−0.09	0.56**	0.18
Node 3 (i) of Element 2: 1st p.v.	0.19	0.19	−0.07	−0.04	−0.23	−0.22	0.03	−0.18	0.84***
a–p	0.01	−0.10	−0.20	0.31	−0.15	−0.47*	−0.13	−0.25	−0.52***
m–l	−0.03	0.50*	0.34	−0.36	0.09	−0.13	0.44*	0.09	−0.09
s–i	−0.12	−0.29	0.22	0.08	0.18	0.24	−0.18	0.33	0.69***
Node 8 (SCH) of Element 2: 1st p.v.	0.11	0.82**	0.27	0.15	−0.01	0.09	−0.11	−0.10	0.11
a–p	0.17	−0.05	0.10	−0.15	−0.80***	−0.05	−0.14	−0.16	0.02
m–l	−0.32	−0.57*	−0.35	−0.12	−0.06	0.14	−0.10	−0.34	−0.05
s–i	0.00	0.01	0.01	0.25	0.81***	0.13	0.08	0.12	−0.04
Node 1 (g) of Element 3: 1st p.v.	−0.79***	−0.19	−0.00	0.19	0.13	−0.00	0.28	−0.10	0.05
a–p	0.69***	−0.01	0.02	0.13	−0.48*	−0.10	0.09	0.18	0.31*
m–l	0.56*	−0.03	0.14	−0.14	0.57**	0.35	−0.04	−0.18	−0.17
s–i	−0.85***	0.03	−0.03	−0.07	−0.13	−0.04	−0.10	−0.00	−0.06
Node 7 (zm) of Element 3: 1st p.v.	−0.07	−0.06	−0.07	−0.09	0.18	0.01	0.91***	−0.08	−0.01
a–p	−0.00	0.34	0.27	0.11	−0.29	0.32	−0.21	−0.57***	−0.13
m–l	−0.08	0.20	0.53*	0.04	0.59*	−0.18	−0.10	0.18	0.24
s–i	−0.09	−0.10	−0.83***	0.10	0.05	−0.08	−0.03	0.26	−0.05
Age	−0.10	0.86***	−0.23	0.15	0.10	0.14	−0.08	−0.13	−0.03

[1] The sample size is 27. The cumulative proportion of the variances of the nine principal components is 81.90%.

[2] p.v.: principal value; a–p: direction cosine for the anterior-posterior axis; m–l: direction cosine for the medial-lateral axis; s–i: direction cosine for the superior-inferior axis.

* $P<0.05$; ** $P<0.01$; *** $P<0.001$, by a two-tailed bootstrap test.

Table 12. Principal component analysis of the correlations between the linearized first principal values and their direction cosines at six craniofacial landmarks, i.e., ft, STH, i, SCH, g, and zm in the three left elements, and age in African-Americans.[1]

Variable[2]	Factor loadings									Total variance (%)
	PC I	II	III	IV	V	VI	VII	VIII	IX	
Node 5 (ft) of Element 1: 1st p.v.	−0.54*	0.44**	−0.24	0.30*	−0.15	0.46***	0.16	−0.18**	0.02	91.85
a–p	0.60***	−0.44	−0.15	0.22	0.05	0.25	0.16	−0.36*	−0.06	85.43
m–l	0.13	−0.39	−0.10	−0.64	0.39	0.04	0.04	−0.05	0.05	74.76
s–i	−0.25	0.22	0.34	0.41	−0.25	−0.00	−0.17	0.50**	0.33*	84.29
Node 6 (STH) of Element 1: 1st p.v.	−0.48	0.52***	0.01	0.18	−0.13	0.55***	−0.03	−0.07	0.08	86.89
a–p	0.66***	−0.35	−0.12	0.31	−0.22	0.28	−0.02	0.22	−0.11	85.16
m–l	0.08	−0.47	−0.04	−0.66*	0.02	0.11	0.01	0.21	0.42**	89.63
s–i	−0.73***	0.13	0.10	0.17	0.41*	0.04	−0.09	−0.27*	0.04	84.53
Node 3 (i) of Element 2: 1st p.v.	−0.29	−0.66***	−0.24***	0.13*	−0.36***	0.17**	0.17**	0.15**	−0.02	80.11
a–p	0.55**	0.15	0.03	0.29	0.40	0.20	−0.31	0.00	−0.32	79.74
m–l	−0.07	−0.33	−0.01	−0.22	0.23	0.64**	−0.41	0.09	0.25	85.89
s–i	−0.32	−0.25	0.20	−0.09	−0.67*	−0.22	0.44*	−0.08	−0.08	91.40
Node 8 (SCH) of Element 2: 1st p.v.	−0.66**	−0.26	−0.10	−0.17	0.22*	0.30**	0.11	0.30*	−0.39**	93.07
a–p	−0.59***	−0.35	−0.04	0.27	0.25	−0.44**	−0.18	−0.08	0.16	86.00
m–l	0.12	−0.32	−0.31	0.21	−0.25	0.34	0.32	−0.39	0.29	77.66
s–i	0.44*	0.68	0.16	−0.32	−0.10	0.31	0.05	−0.07	−0.02	89.66
Node 1 (g) of Element 3: 1st p.v.	−0.06	−0.06	0.80***	−0.05	−0.18	0.26*	−0.10	−0.24*	−0.01	81.21
a–p	−0.16	−0.25	−0.72*	0.31	0.05	0.13	−0.31	0.08	0.04	82.27
m–l	−0.25	0.39	−0.48	−0.51	−0.07	−0.00	0.02	−0.30	−0.10	79.80
s–i	0.23	−0.06	0.76*	0.24	0.19	0.13	0.14	0.00	0.15	78.54
Node 7 (zm) of Element 3: 1st p.v.	−0.25	−0.39***	0.46***	−0.40***	−0.11*	0.18**	−0.18**	−0.24***	−0.13*	74.21
a–p	0.13	−0.35	0.06	0.42	0.50*	0.06	0.49*	0.05	−0.01	81.83
m–l	−0.06	−0.46	0.09	0.03	−0.62	0.10	−0.43	0.08	−0.30	89.05
s–i	0.41*	0.53	−0.33	−0.19	−0.27	0.03	0.07	0.29	0.11	76.32
Age	−0.31	0.08	0.12	−0.21	0.26	0.30	0.49	0.48*	−0.17	81.66
Total contribution (%)	15.58	14.37	11.07	10.15	9.21	7.72	6.25	5.59	3.71	83.64
Cumulative proportion (%)	15.58	29.95	41.02	51.17	60.37	68.09	74.34	79.93	83.64	83.64

[1] The sample size is 27. The number of principal components shown here was determined so that the cumulative proportion of the variances of the principal components exceeded 80%.

[2] p.v.: principal value; a-p: direction cosine for the anterior-posterior axis; m–l: direction cosine for the medial-lateral axis; s–i: direction cosine for the superior-inferior axis.

* $P<0.05$; ** $P<0.01$; *** $P<0.001$, by a two-tailed bootstrap test.

Table 13. Rotated solution of the first nine principal components extracted from the correlations between the linearized first principal values and their direction cosines at six craniofacial landmarks, i.e., ft, STH, i, SCH, g, and zm in the three left elements, and age in African-Americans.[1]

Variable[2]	Factor loadings								
	Fac I	II	III	IV	V	VI	VII	VIII	IX
Node 5 (ft) of Element 1: 1st p.v.	0.04	−0.02	−0.14	0.16	−0.11	0.92***	0.05	−0.01	−0.13
a–p	0.83***	0.06	0.06	−0.03	0.22	−0.21	−0.05	−0.20	0.16
m–l	0.03	−0.04	0.02	−0.56	0.02	−0.40*	0.14	−0.46**	−0.18
s–i	−0.28	−0.02	0.06	0.06	−0.09	0.23	−0.07	0.83***	0.02
Node 6 (STH) of Element 1: 1st p.v.	−0.14	0.10	0.06	−0.00	0.01	0.90***	0.01	0.11	−0.10
a–p	0.63***	0.33	−0.11	−0.00	0.25	−0.28	−0.35	0.28	0.02
m–l	0.02	0.10	−0.01	−0.80	−0.31	−0.37	0.01	−0.07	−0.08
s–i	−0.27	−0.65***	0.12	0.01	0.07	0.51**	0.22	−0.10	−0.11
Node 3 (i) of Element 2: 1st p.v.	0.42	−0.28	−0.23	−0.16	−0.44	0.01	−0.44	0.11	−0.25
a–p	0.17	0.16	0.04	0.15	0.84***	−0.10	−0.01	0.01	0.04
m–l	0.11	−0.09	0.07	−0.81**	0.29	0.20	−0.20	0.04	−0.10
s–i	0.07	−0.03	0.22	0.26	−0.84***	−0.03	−0.28	−0.01	−0.09
Node 8 (SCH) of Element 2: 1st p.v.	−0.15	−0.35	−0.10	−0.18	−0.06	0.21	−0.24	−0.16	−0.78***
a–p	−0.18	−0.87***	−0.16	0.01	−0.14	−0.04	0.04	0.11	0.08
m–l	0.75***	0.00	−0.10	−0.13	−0.29	0.24	0.02	−0.09	0.20
s–i	−0.16	0.81*	0.26	0.02	0.20	0.20	0.19	−0.15	0.10
Node 1 (g) of Element 3: 1st p.v.	−0.03	−0.01	0.85***	−0.08	−0.04	0.14	−0.21	0.11	0.07
a–p	0.23	−0.30	−0.72**	−0.16	0.18	0.20	−0.25	0.03	0.06
m–l	−0.32	0.20	−0.31	−0.05	−0.18	0.31	0.08	−0.64***	0.06
s–i	0.18	−0.03	0.71***	0.02	0.17	−0.12	0.22	0.39*	−0.04
Node 7 (zm) of Element 3: 1st p.v.	−0.10	−0.22	0.57	−0.34	−0.16	−0.04	−0.38	−0.26	−0.06
a–p	0.57*	−0.32	0.07	0.13	0.16	−0.19	0.39	0.15	−0.37
m–l	0.04	−0.06	0.07	−0.05	−0.14	−0.08	−0.91***	0.10	0.09
s–i	−0.13	0.76	−0.37	0.04	−0.01	0.01	0.12	0.08	0.10
Age	−0.10	0.11	0.07	−0.09	−0.10	0.11	0.21	0.06	−0.84***

[1] The sample size is 27. The cumulative proportion of the variances of the nine principal components is 83.64%.
[2] p.v.: principal value; a–p: direction cosine for the anterior-posterior axis; m–l: direction cosine for the medial-lateral axis; s–i: direction cosine for the superior-inferior axis.
* $P<0.05$; ** $P<0.01$; *** $P<0.001$, by a two-tailed bootstrap test.

Table 14. Principal component analysis of the correlations between the linearized first principal values and their direction cosines at six craniofacial landmarks, i.e., b, ba, l, ast, fmt, and n in the three right elements, and the degree of occlusal wear on the maxillary first molar in early modern Japanese.[1]

Variable[2]	Factor loadings											Total variance (%)
	PC I	II	III	IV	V	VI	VII	VIII	IX	X	XI	
Node 3 (b) of Element 1: 1st p.v.	−0.05	0.84***	0.03	0.16**	0.19**	−0.15*	0.18**	−0.06	0.07	0.19***	0.07	87.56
a–p	0.26	−0.45	0.18	−0.37	0.02	−0.14	−0.22	−0.43*	−0.08	−0.15	0.16	74.11
m–l	−0.03	0.09	−0.28	−0.04	−0.33	0.05	0.24	−0.00	−0.71***	−0.18	−0.26	86.53
s–i	0.07	−0.32	0.12	0.26	−0.31	0.38	0.11	0.57*	0.38*	0.08	0.11	93.03
Node 4 (ba) of Element 1: 1st p.v.	−0.22	0.82***	0.17***	−0.02	0.04	−0.04	−0.16***	−0.05	0.03	0.16***	0.14***	83.02
a–p	−0.76***	−0.17	0.29	−0.06	−0.24	0.12	−0.08	−0.25*	0.04	0.07	−0.25**	89.96
m–l	0.37*	0.05	0.06	−0.59*	0.02	−0.32	−0.02	0.15	0.19	−0.07	0.16	68.60
s–i	0.25	−0.08	0.04	0.68*	0.18	0.10	−0.03	0.18	−0.12	−0.24	0.46***	88.19
Node 4 (l) of Element 2: 1st p.v.	0.03	0.60***	−0.39***	−0.00	0.09*	0.27***	−0.25***	−0.14**	0.21***	−0.14**	−0.17***	77.12
a–p	−0.06	0.10	0.58	−0.13	−0.03	0.42	0.21	−0.29	0.14	−0.31	−0.07	78.48
m–l	−0.34*	0.12	−0.07	0.23	0.04	−0.65**	0.44	−0.17	−0.09	−0.03	0.17	86.33
s–i	0.46**	−0.27	−0.41	0.24	−0.10	−0.10	−0.41*	−0.23	0.06	0.06	−0.08	76.58
Node 7 (ast) of Element 2: 1st p.v.	−0.18	0.05	0.01	−0.46***	0.41***	0.34***	−0.33***	0.34***	−0.33***	−0.05	−0.10**	87.39
a–p	0.40*	0.24	0.12	−0.11	0.65**	−0.13	−0.16	0.32	−0.10	−0.19	−0.13	87.35
m–l	0.02	−0.07	−0.05	−0.43	−0.05	0.54**	0.25	−0.08	−0.24	0.31	0.41**	87.35
s–i	−0.51***	−0.30	−0.21	−0.17	−0.16	−0.44*	−0.16	0.30	0.24	−0.19	−0.14	86.68
Node 2 (fmt) of Element 3: 1st p.v.	−0.39	0.14*	−0.36***	0.12**	0.05	0.22***	−0.44***	−0.36***	0.16***	−0.24***	0.27***	83.79
a–p	−0.24	0.44	0.35	−0.23	−0.51*	−0.17	−0.26	0.30	−0.05	0.11	0.02	88.58
m–l	0.59***	0.06	0.05	−0.21	0.24	0.06	0.48*	−0.12	0.27	−0.21	−0.25	87.88
s–i	−0.52***	−0.36	−0.25	0.03	0.61**	−0.09	−0.01	0.05	−0.18	0.16	0.06	90.28
Node 5 (n) of Element 3: 1st p.v.	−0.56**	−0.05	0.47***	−0.16	0.16	−0.06	0.02	0.04	0.02	−0.48***	0.22**	87.42
a–p	0.59***	0.24	−0.16	−0.19	−0.47*	−0.09	−0.17	0.01	−0.14	−0.20	0.12	80.18
m–l	0.25	−0.20	0.61	0.09	0.28	−0.09	−0.26	−0.19	0.05	0.42**	−0.16	88.22
s–i	−0.35*	0.05	−0.64	−0.19	0.16	0.24	0.25	0.05	0.28	0.01	−0.10	80.45
Occlusal wear of UM1	−0.03	0.09	0.29	0.68***	−0.01	0.18	−0.09	0.06	−0.17	−0.19	−0.27*	73.27
Total contribution (%)	13.48	11.15	9.52	9.14	8.10	7.20	6.17	5.64	5.12	4.37	4.05	83.93
Cumulative proportion (%)	13.48	24.63	34.15	43.29	51.38	58.59	64.75	70.40	75.52	79.89	83.93	83.93

[1] The sample size is 33. The number of principal components shown here was determined so that the cumulative proportion of the variances of the principal components exceeded 80%.

[2] p.v.: principal value; a–p: direction cosine for the anterior-posterior axis; m–l: direction cosine for the medial-lateral axis; s–i: direction cosine for the superior-inferior axis.

* $P<0.05$; ** $P<0.01$; *** $P<0.001$, by a two-tailed bootstrap test.

Table 15. Rotated solution of the first eleven principal components extracted from the correlations between the linearized first principal values and their direction cosines at six craniofacial landmarks, i.e., b, ba, l, ast, fmt, and n in the three right elements, and the degree of occlusal wear on the maxillary first molar in early modern Japanese.[1]

Variable[2]	Factor loadings										
	Fac I	II	III	IV	V	VI	VII	VIII	IX	X	XI
Node 3 (b) of Element 1: 1st p.v.	0.00	0.91***	−0.02	0.01	0.11	−0.11	0.00	−0.15	−0.00	−0.00	0.08
a–p	0.16	−0.57**	−0.09	−0.32	0.04	−0.02	0.09	−0.36*	0.36	0.11	0.01
m–l	0.22	−0.11	0.28	0.35	−0.09	0.07	−0.11	−0.40**	−0.62***	0.16	−0.11
s–i	0.07	−0.19	0.13	0.11	−0.05	−0.05	0.01	0.91***	−0.03	0.05	0.13
Node 4 (ba) of Element 1: 1st p.v.	0.15	0.82**	−0.19	−0.02	−0.20	0.07	0.15	−0.14	0.09	0.03	−0.06
a–p	−0.20	−0.11	−0.12	0.30	−0.35	−0.15	0.45*	0.01	0.09	−0.01	−0.62***
m–l	0.27	−0.02	0.16	−0.73***	0.15	0.15	0.02	−0.05	0.07	−0.08	0.01
s–i	−0.02	−0.05	−0.06	0.30	−0.02	−0.08	−0.02	0.16	0.05	−0.00	0.87***
Node 4 (l) of Element 2: 1st p.v.	0.16	0.44	−0.59	0.08	0.21	0.24	−0.20	−0.04	−0.20	−0.07	−0.11
a–p	0.23	−0.01	−0.10	0.21	0.36*	−0.01	0.66***	0.05	0.19	0.22	−0.17
m–l	−0.31	0.25	0.23	−0.08	−0.10	−0.59***	0.15	−0.38	−0.20	−0.24	0.13
s–i	0.16	−0.35	−0.29	0.03	0.03	−0.08	−0.67***	−0.08	0.16	−0.15	0.13
Node 7 (ast) of Element 2: 1st p.v.	−0.19	−0.01	−0.04	−0.07	−0.14	0.86***	0.15	−0.07	−0.07	0.15	−0.08
a–p	−0.03	0.21	0.16	−0.16	0.34	0.63***	−0.03	−0.17	0.18	−0.26	0.37*
m–l	−0.04	−0.07	0.03	−0.20	−0.03	0.10	0.06	0.07	−0.12	0.89***	−0.07
s–i	−0.23	−0.24	−0.01	−0.29	−0.37	−0.05	0.12	0.13	−0.28	−0.59***	−0.28
Node 2 (fmt) of Element 3: 1st p.v.	−0.12	0.03	−0.86***	0.07	−0.23	−0.03	0.07	−0.10	−0.11	0.00	0.04
a–p	0.47	0.38	0.17	−0.11	−0.56**	0.09	0.23	0.11	0.00	−0.11	−0.28
m–l	0.16	−0.02	0.16	−0.18	0.89***	0.00	−0.01	−0.01	0.02	0.01	0.02
s–i	−0.88***	−0.13	−0.03	−0.02	−0.20	0.16	0.01	−0.17	−0.05	−0.02	0.06
Node 5 (n) of Element 3: 1st p.v.	−0.16	−0.05	−0.06	−0.06	−0.18	0.06	0.88***	−0.07	0.00	−0.16	0.05
a–p	0.77***	−0.05	−0.01	−0.23	0.00	0.03	−0.28	−0.13	−0.17	0.04	0.16
m–l	−0.06	−0.04	0.22	0.10	0.05	0.08	−0.05	−0.06	0.90***	0.00	−0.05
s–i	−0.45	0.10	−0.33	−0.15	0.20	0.03	−0.11	0.18	−0.54***	0.06	−0.29*
Occlusal wear of UM1	0.09	0.07	0.04	0.77**	−0.01	0.03	0.09	0.08	0.11	−0.22	0.22

[1] The sample size is 33. The cumulative proportion of the variances of the eleven principal components is 83.93%.

[2] p.v.: principal value; a–p: direction cosine for the anterior-posterior axis; m–l: direction cosine for the medial-lateral axis; s–i: direction cosine for the superior-inferior axis.

* $P<0.05$; ** $P<0.01$; *** $P<0.001$, by a two-tailed bootstrap test.

Table 16. Principal component analysis of the correlations between the linearized first principal values and their direction cosines at six craniofacial landmarks, i.e., b, ba, l, ast, fmt, and n in the three left elements, and the degree of occlusal wear on the maxillary first molar in early modern Japanese.[1]

Variable[2]	Factor loadings											Total variance (%)
	PC I	II	III	IV	V	VI	VII	VIII	IX	X	XI	
Node 3 (b) of Element 1: 1st p.v.	−0.49*	0.45***	0.21**	0.24***	−0.31***	0.17***	0.21***	−0.09*	0.32***	0.06	−0.10*	84.53
a–p	0.52***	0.27	0.04	−0.37	−0.41	−0.01	−0.31	0.04	−0.10	0.03	−0.18	79.04
m–l	−0.10	0.24	0.48*	0.16	0.51	−0.19	0.18	−0.29	0.03	−0.03	−0.21	77.50
s–i	0.02	−0.18	−0.24	0.45	−0.02	0.07	0.51*	0.33	−0.05	−0.02	0.49***	90.12
Node 4 (ba) of Element 1: 1st p.v.	0.37	0.35***	0.02	−0.06	−0.42***	0.43***	0.11***	−0.04	0.11***	−0.10***	0.27***	72.45
a–p	0.33	0.29	−0.39	−0.13	0.14	−0.48*	0.22	0.20	0.21	−0.22	0.08	80.08
m–l	0.65***	0.11	0.25	0.26	0.18	0.15	0.12	0.16	−0.09	0.12	0.13	69.46
s–i	−0.63***	−0.11	0.13	0.07	−0.36	0.35	−0.18	−0.05	−0.18	0.16	0.23	82.99
Node 4 (l) of Element 2: 1st p.v.	−0.24	0.30***	−0.09	−0.11*	−0.01	0.52***	0.16***	0.14***	0.43***	−0.46***	−0.15***	90.06
a–p	0.16	−0.01	0.62	−0.13	−0.27	−0.24	−0.17	0.24	−0.38	−0.27	0.13	87.64
m–l	0.05	0.13	−0.07	0.68**	−0.16	−0.53*	0.14	−0.05	0.02	0.11	−0.12	84.74
s–i	0.22	−0.45	−0.23	−0.29	0.39	0.50	−0.03	−0.13	−0.08	0.15	0.10	84.27
Node 7 (ast) of Element 2: 1st p.v.	0.29	−0.13*	−0.11*	−0.49***	0.08	0.19***	0.46***	0.26***	−0.12*	0.01	−0.33***	79.92
a–p	−0.27	0.29	−0.47	−0.07	−0.40	−0.12	0.27	−0.38*	−0.31	−0.19	0.01	91.50
m–l	0.46**	−0.31	0.49	0.33	0.23	0.18	0.06	−0.16	0.24	−0.06	0.07	84.57
s–i	−0.21	0.22	−0.20	−0.03	−0.00	−0.08	−0.54	0.32	0.37	0.39*	0.06	82.59
Node 2 (fmt) of Element 3: 1st p.v.	0.51*	0.21***	−0.05	0.23***	−0.11**	0.08	−0.50***	−0.22***	0.12***	−0.38***	0.13***	84.57
a–p	0.41**	−0.03	0.05	−0.49	−0.12	−0.37	0.06	−0.34	0.34*	0.17	0.22	87.00
m–l	0.11	−0.50	0.23	0.26	−0.47	0.00	−0.04	0.38*	0.05	−0.14	−0.32*	87.58
s–i	−0.26	0.35	−0.05	0.23	0.53*	0.20	−0.33	0.00	−0.21	−0.19	−0.05	76.11
Node 5 (n) of Element 3: 1st p.v.	−0.08	0.72***	0.40***	−0.24	0.22*	−0.06	0.06	0.04	−0.16*	−0.09	0.18***	86.57
a–p	−0.06	−0.60	−0.39	0.07	0.06	−0.13	−0.18	−0.30	−0.03	−0.32*	−0.00	76.58
m–l	−0.55***	−0.16	0.44	−0.47	0.01	−0.20	0.17	−0.01	0.09	−0.05	0.15	84.60
s–i	0.39*	0.63	−0.25	0.18	−0.03	0.23	0.08	−0.08	−0.22	0.30*	−0.15	86.91
Occlusal wear of UM1	0.18	−0.21	0.31*	0.10	−0.32**	0.22	0.19	−0.44***	0.04	0.14	−0.10	60.13
Total contribution (%)	12.53	11.63	9.02	8.75	8.10	7.69	6.69	5.25	4.50	4.27	3.63	82.06
Cumulative proportion (%)	12.53	24.15	33.18	41.93	50.03	57.72	64.41	69.66	74.16	78.43	82.06	82.06

[1] The sample size is 33. The number of principal components shown here was determined so that the cumulative proportion of the variances of the principal components exceeded 80%.

[2] p.v.: principal value; a–p: direction cosine for the anterior-posterior axis; m–l: direction cosine for the medial-lateral axis; s–i: direction cosine for the superior-inferior axis.

* $P<0.05$; ** $P<0.01$; *** $P<0.001$, by a two-tailed bootstrap test.

Table 17. Rotated solution of the first eleven principal components extracted from the correlations between the linearized first principal values and their direction cosines at six craniofacial landmarks, i.e., b, ba, l, ast, fmt, and n in the three left elements, and the degree of occlusal wear on the maxillary first molar in early modern Japanese.[1]

Variable[2]	Factor loadings										
	Fac I	II	III	IV	V	VI	VII	VIII	IX	X	XI
Node 3 (b) of Element 1: 1st p.v.	0.02	0.19	−0.10	0.56	−0.01	0.39	0.12	0.06	0.54*	0.13	0.02
a–p	0.46	−0.11	−0.11	−0.13	−0.43*	−0.13	−0.11	0.12	0.02	−0.44*	0.33
m–l	−0.16	0.51*	0.37	0.33	−0.25	−0.07	0.12	−0.32	−0.05	0.11	−0.21
s–i	0.05	−0.13	0.04	0.07	0.92***	−0.06	0.07	−0.09	0.00	0.08	−0.04
Node 4 (ba) of Element 1: 1st p.v.	0.48*	0.07	−0.02	−0.11	0.17	0.11	−0.23	−0.07	0.46	−0.21	0.35
a–p	0.06	0.11	−0.16	0.12	0.16	−0.82***	−0.05	0.11	0.04	0.01	0.15
m–l	0.49	0.08	0.55*	−0.05	0.22	−0.15	−0.03	−0.13	−0.10	−0.19	0.03
s–i	−0.18	−0.03	−0.26	−0.01	0.14	0.82***	0.00	0.15	0.07	−0.07	−0.09
Node 4 (l) of Element 2: 1st p.v.	−0.05	0.02	−0.06	−0.09	−0.02	−0.05	−0.01	0.00	0.91***	0.12	−0.18
a–p	−0.12	−0.00	0.11	0.08	−0.07	0.06	−0.06	−0.12	−0.15	−0.89***	0.04
m–l	0.16	−0.15	0.01	0.79***	0.17	−0.15	−0.08	−0.06	−0.30	0.13	−0.04
s–i	0.05	−0.05	0.18	−0.81***	0.04	0.08	0.03	−0.10	−0.12	0.33	−0.00
Node 7 (ast) of Element 2: 1st p.v.	0.17	−0.16	−0.02	−0.43	−0.07	−0.34	0.58*	−0.24	0.16	−0.06	0.11
a–p	0.12	0.09	−0.86***	0.17	0.06	0.02	−0.07	−0.30	0.06	0.10	0.07
m–l	0.00	−0.07	0.81***	−0.02	0.06	0.04	−0.22	−0.34	−0.01	0.04	0.11
s–i	0.02	0.01	−0.01	0.09	−0.13	0.05	−0.05	0.88***	0.01	0.12	−0.02
Node 2 (fmt) of Element 3: 1st p.v.	0.31	−0.06	0.14	−0.00	−0.15	−0.15	−0.81***	−0.00	0.10	−0.13	0.02
a–p	−0.08	0.18	0.04	−0.10	−0.19	−0.28	−0.11	0.02	−0.15	0.02	0.82***
m–l	−0.08	−0.80***	0.23	0.19	0.01	0.12	0.09	−0.07	0.06	−0.32	0.00
s–i	0.05	0.37*	0.03	−0.04	−0.11	0.04	−0.21	0.10	0.04	0.10	−0.74***
Node 5 (n) of Element 3: 1st p.v.	0.08	0.78**	−0.00	0.11	−0.10	−0.07	0.09	0.03	0.19	−0.40	−0.10
a–p	−0.38***	−0.41*	−0.19	−0.21	0.01	−0.09	−0.39*	−0.21	−0.27	0.30*	−0.09
m–l	−0.72*	0.28	−0.07	−0.01	−0.08	0.20	0.33*	−0.01	0.09	−0.21	0.20
s–i	0.88***	0.24	−0.10	0.09	−0.05	−0.06	0.03	−0.01	0.02	0.11	−0.05
Occlusal wear of UM1	0.13	−0.14	0.20	0.08	−0.12	0.39	−0.02	−0.44	0.01	0.09	0.38

[1] The sample size is 33. The cumulative proportion of the variances of the eleven principal components is 82.06%.
[2] p.v.: principal value; a–p: direction cosine for the anterior-posterior axis; m–l: direction cosine for the medial-lateral axis; s–i: direction cosine for the superior-inferior axis.
* $P<0.05$; ** $P<0.01$; *** $P<0.001$, by a two-tailed bootstrap test.

Table 18. Principal component analysis of the correlations between the linearized first principal values and their direction cosines at six craniofacial landmarks, i.e., b, ba, l, ast, fmt, and n in the three right elements, and the degree of occlusal wear on the maxillary first molar in Indians.[1]

Variable[2]	Factor loadings										Total variance (%)
	PC I	II	III	IV	V	VI	VII	VIII	IX	X	
Node 3 (b) of Element 1: 1st p.v.	0.34	0.32	0.58	0.05	−0.24	0.31	−0.21	0.06	0.02	−0.18	79.09
a–p	0.55	0.03	−0.05	−0.12	0.63*	−0.27	−0.09	0.08	0.07	0.19	85.54
m–l	−0.43	−0.03	0.47	0.01	0.31	−0.18	0.05	0.41	0.28	0.05	79.27
s–i	−0.37	−0.23	−0.21	−0.17	−0.49	0.32	0.21	−0.43	−0.09	0.13	86.35
Node 4 (ba) of Element 1: 1st p.v.	−0.09	0.58	0.47	−0.21	−0.02	0.44	−0.16	−0.04	0.02	0.10	84.72
a–p	0.40	0.11	−0.51	−0.18	−0.10	−0.01	−0.61*	−0.11	−0.02	0.23	90.89
m–l	−0.52	0.18	0.37	−0.09	−0.10	−0.60*	0.17	−0.10	0.14	−0.19	90.90
s–i	0.14	−0.38	0.12	0.43	0.22	0.42	0.12	0.41	−0.10	0.15	80.75
Node 4 (l) of Element 2: 1st p.v.	−0.04	0.57	0.44	0.48	−0.14	0.16	−0.01	0.04	−0.06	0.08	80.57
a–p	0.06	−0.74	0.25	−0.17	−0.16	0.31	−0.04	0.10	0.21	0.14	84.38
m–l	0.60	−0.01	−0.01	−0.07	−0.08	−0.54	−0.11	0.24	−0.05	−0.11	74.91
s–i	−0.32	0.52	−0.25	−0.33	0.24	−0.04	−0.04	−0.06	0.05	0.16	64.34
Node 7 (ast) of Element 2: 1st p.v.	0.16	0.20	0.66	0.32	0.22	−0.09	−0.04	−0.44*	−0.10	0.07	87.57
a–p	0.09	0.43	−0.32	0.41	−0.24	−0.07	0.43	0.05	0.14	0.09	74.10
m–l	0.06	−0.43	0.23	0.27	−0.37	−0.38	−0.27	−0.26	−0.33	−0.07	85.21
s–i	0.08	0.12	0.21	−0.76*	0.33	0.09	0.06	−0.16	−0.21	−0.01	83.66
Node 2 (fmt) of Element 3: 1st p.v.	−0.44	0.20	−0.05	0.23	0.18	−0.17	−0.11	0.15	−0.56*	0.43	87.38
a–p	0.66	0.45	−0.13	0.05	0.00	0.13	−0.10	−0.11	0.25	−0.25	81.74
m–l	−0.16	−0.49	0.55	−0.23	0.35	−0.02	−0.09	−0.25	0.15	0.06	84.32
s–i	−0.39	−0.00	0.02	−0.47	−0.52	−0.05	−0.13	0.42*	−0.02	−0.09	84.76
Node 5 (n) of Element 3: 1st p.v.	−0.56	0.36	−0.11	−0.13	0.04	0.16	−0.38	0.18	−0.05	−0.14	69.00
a–p	0.60	−0.16	0.16	−0.22	0.03	0.19	0.17	0.21	−0.47*	−0.19	82.03
m–l	0.47	0.11	0.13	−0.28	−0.34	−0.10	0.26	−0.01	0.32	0.48*	85.06
s–i	−0.28	−0.30	−0.27	0.43	0.24	0.15	−0.45	−0.11	0.33	−0.06	83.92
Occlusal wear of UM1	−0.16	0.04	−0.40	−0.04	0.54	0.21	0.36	−0.14	−0.09	−0.25	74.42
Total contribution (%)	14.04	12.02	11.22	9.07	8.85	7.20	5.78	5.21	4.81	3.61	81.79
Cumulative proportion (%)	14.04	26.06	37.28	46.35	55.19	62.39	68.17	73.38	78.19	81.79	81.79

[1] The sample size is 35. The number of principal components shown here was determined so that the cumulative proportion of the variances of the principal components exceeded 80%.

[2] p.v.: principal value; a–p: direction cosine for the anterior-posterior axis; m–l: direction cosine for the medial-lateral axis; s–i: direction cosine for the superior-inferior axis.

* $P<0.05$; ** $P<0.01$; *** $P<0.001$, by a two-tailed bootstrap test.

Table 19. Rotated solution of the first ten principal components extracted from the correlations between the linearized first principal values and their direction cosines at six craniofacial landmarks, i.e., b, ba, l, ast, fmt, and n in the three right elements, and the degree of occlusal wear on the maxillary first molar in Indians.[1]

Variable[2]	Factor loadings									
	Fac I	II	III	IV	V	VI	VII	VIII	IX	X
Node 3 (b) of Element 1: 1st p.v.	0.04	−0.09	0.80*	−0.03	0.10	−0.14	0.17	0.04	0.27	0.05
a–p	0.20	−0.04	−0.18	−0.19	0.72***	0.22	0.10	−0.37	−0.02	0.17
m–l	−0.70**	−0.07	0.11	−0.26	0.27	0.16	−0.25	0.18	−0.17	0.03
s–i	0.12	0.08	−0.17	−0.03	−0.89***	−0.05	0.01	0.09	0.00	0.10
Node 4 (ba) of Element 1: 1st p.v.	0.00	0.12	0.80*	−0.15	−0.12	0.36*	0.09	0.08	−0.06	0.06
a–p	0.89***	0.15	−0.07	−0.01	0.21	−0.01	−0.14	0.12	−0.04	0.12
m–l	−0.68**	0.63***	0.02	−0.03	−0.00	−0.16	−0.08	0.11	−0.09	0.01
s–i	−0.11	−0.87***	0.02	−0.01	0.06	−0.02	−0.02	−0.11	−0.10	−0.08
Node 4 (l) of Element 2: 1st p.v.	−0.19	−0.03	0.76**	0.36	−0.01	−0.05	−0.08	−0.15	−0.19	−0.01
a–p	−0.05	−0.52	−0.13	−0.54*	−0.22	−0.20	−0.07	0.18	0.26	0.28
m–l	0.15	0.11	−0.14	0.12	0.64**	−0.36	0.26	0.08	0.15	0.20
s–i	0.08	0.45*	0.02	0.04	0.01	0.58**	−0.08	0.09	−0.27	−0.03
Node 7 (ast) of Element 2: 1st p.v.	−0.20	0.13	0.53	−0.17	0.10	−0.24	0.02	−0.66***	−0.10	0.03
a–p	−0.06	0.03	−0.01	0.82***	−0.06	0.11	−0.06	−0.14	0.01	0.18
m–l	0.04	0.08	−0.05	−0.14	−0.08	−0.89***	0.00	−0.08	−0.11	−0.05
s–i	0.06	0.28	0.05	−0.54	0.03	0.41	0.54**	−0.03	−0.00	0.03
Node 2 (fmt) of Element 3: 1st p.v.	−0.04	0.02	0.02	0.11	0.00	0.01	−0.04	0.00	−0.91***	−0.16
a–p	0.41	0.10	0.30	0.32	0.33	0.15	0.08	−0.21	0.51*	0.04
m–l	−0.33	−0.03	−0.02	−0.82***	−0.03	−0.07	−0.09	−0.23	0.05	0.06
s–i	−0.12	0.17	0.03	−0.08	−0.17	−0.05	0.09	0.87***	−0.05	0.07
Node 5 (n) of Element 3: 1st p.v.	0.03	0.23	0.24	−0.03	−0.08	0.30	−0.24	0.45	−0.24	−0.41
a–p	0.18	−0.35*	0.04	−0.10	0.18	−0.12	0.76***	−0.03	0.15	−0.04
m–l	0.09	0.05	0.08	0.08	0.04	0.04	0.18	−0.01	0.17	0.87***
s–i	0.14	−0.20	−0.15	−0.13	−0.02	−0.03	−0.78***	−0.09	0.05	−0.36
Occlusal wear of UM1	−0.05	−0.02	−0.37	0.08	−0.11	0.53**	0.12	−0.30	0.05	−0.45*

[1] The sample size is 35. The cumulative proportion of the variances of the ten principal components is 81.79%.

[2] p.v.: principal value; a–p: direction cosine for the anterior-posterior axis; m–l: direction cosine for the medial-lateral axis; s–i: direction cosine for the superior-inferior axis.

* $P<0.05$; ** $P<0.01$; *** $P<0.001$, by a two-tailed bootstrap test.

Table 20. Principal component analysis of the correlations between the linearized first principal values and their direction cosines at six craniofacial landmarks, i.e., b, ba, l, ast, fmt, and n in the three left elements, and the degree of occlusal wear on the maxillary first molar in Indians.[1]

Variable[2]	Factor loadings											Total variance (%)
	PC I	II	III	IV	V	VI	VII	VIII	IX	X	XI	
Node 3 (b) of Element 1: 1st p.v.	0.29	0.71	−0.33	0.14	0.21	0.05	0.18	−0.12	0.05	0.01	0.16	82.99
a–p	0.51	−0.52	0.12	0.22	0.14	−0.30	−0.01	−0.17	−0.27	0.01	−0.07	81.00
m–l	0.11	0.30	−0.10	−0.04	−0.25	−0.38	−0.33	−0.24	0.32	−0.36	0.17	74.28
s–i	−0.67	0.33	−0.05	−0.17	0.02	0.39	0.26	0.06	0.15	0.03	0.32*	93.19
Node 4 (ba) of Element 1: 1st p.v.	0.46	0.61	−0.12	0.29	0.10	0.09	−0.01	−0.29	−0.07	0.22	0.12	85.21
a–p	−0.04	−0.06	−0.29	0.23	−0.18	−0.33	0.28	0.51	0.15	0.36	0.34	88.13
m–l	0.57	−0.06	0.43	0.41	0.01	0.32	0.10	−0.15	−0.06	−0.13	−0.03	83.80
s–i	−0.51	0.05	−0.28	−0.33	0.33	0.22	−0.10	−0.43*	0.12	0.03	−0.08	82.61
Node 4 (l) of Element 2: 1st p.v.	0.25	0.61	−0.13	−0.33	−0.31	−0.03	−0.18	−0.09	0.18	−0.02	−0.33*	84.11
a–p	0.06	−0.20	−0.15	−0.40	0.66*	0.16	0.31	0.12	−0.01	−0.01	−0.04	79.14
m–l	−0.27	0.05	−0.34	0.36	0.30	−0.25	−0.28	−0.07	−0.36	−0.01	0.25	75.29
s–i	0.18	0.01	0.64	0.06	−0.12	0.36	0.05	0.16	0.46*	0.01	0.11	84.72
Node 7 (ast) of Element 2: 1st p.v.	0.67	0.38	−0.16	−0.19	0.05	0.03	0.27	0.03	−0.05	0.18	0.01	75.55
a–p	0.01	−0.11	0.16	0.43	0.30	0.02	−0.39	0.05	0.38	0.40	−0.01	77.43
m–l	0.44	−0.12	−0.18	−0.46	0.12	0.20	−0.19	0.03	−0.07	−0.34	0.49*	90.62
s–i	−0.59	0.24	0.11	0.20	−0.17	−0.30	0.39	−0.22	0.04	−0.08	−0.20	82.46
Node 2 (fmt) of Element 3: 1st p.v.	−0.04	0.33	−0.07	0.09	0.29	−0.38	−0.32	0.52*	0.11	−0.30	−0.13	84.36
a–p	−0.08	−0.32	−0.34	0.16	−0.60	0.26	−0.34	0.08	0.07	−0.07	0.13	82.91
m–l	0.34	−0.02	−0.17	−0.56	0.18	−0.20	−0.29	0.12	0.22	0.33	−0.15	81.55
s–i	−0.06	0.36	0.28	0.38	0.53	0.09	0.03	0.32	0.08	−0.36	−0.09	89.26
Node 5 (n) of Element 3: 1st p.v.	−0.18	0.64	0.38	−0.03	−0.19	−0.21	−0.07	0.04	−0.32	0.19	0.14	82.90
a–p	−0.10	−0.17	−0.75	0.38	0.18	0.17	−0.01	−0.10	0.17	0.02	−0.15	86.71
m–l	0.01	−0.26	0.25	−0.45	0.08	−0.57	0.34	−0.12	0.17	−0.07	0.14	84.03
s–i	−0.33	0.19	0.37	−0.36	0.07	0.24	−0.43	0.20	−0.41*	0.17	−0.06	90.45
Occlusal wear of UM1	−0.19	−0.08	0.48	0.07	0.35	−0.20	−0.28	−0.44	0.21	0.14	0.26	84.89
Total contribution (%)	12.31	11.49	10.06	9.45	8.04	7.03	6.49	5.67	4.86	4.27	3.84	83.50
Cumulative proportion (%)	12.31	23.80	33.86	43.32	51.35	58.38	64.87	70.55	75.40	79.67	83.50	83.50

[1] The sample size is 35. The number of principal components shown here was determined so that the cumulative proportion of the variances of the principal components exceeded 80%.

[2] p.v.: principal value; a–p: direction cosine for the anterior-posterior axis; m–l: direction cosine for the medial-lateral axis; s–i: direction cosine for the superior-inferior axis.

* $P<0.05$; ** $P<0.01$; *** $P<0.001$, by a two-tailed bootstrap test.

Table 21. Rotated solution of the first eleven principal components extracted from the correlations between the linearized first principal values and their direction cosines at six craniofacial landmarks, i.e., b, ba, l, ast, fmt, and n in the three left elements, and the degree of occlusal wear on the maxillary first molar in Indians.[1]

Variable[2]	Factor loadings										
	Fac I	II	III	IV	V	VI	VII	VIII	IX	X	XI
Node 3 (b) of Element 1: 1st p.v.	−0.19	0.85*	−0.08	0.10	0.18	−0.11	0.02	0.04	−0.02	−0.07	0.04
a–p	0.83**	−0.05	−0.13	−0.13	−0.12	−0.11	0.08	−0.02	0.17	0.12	0.11
m–l	−0.02	0.12	−0.03	0.82***	0.10	−0.06	−0.08	−0.06	0.12	0.03	0.09
s–i	−0.92***	−0.00	0.10	−0.13	−0.03	0.03	0.24	0.05	0.01	−0.01	−0.05
Node 4 (ba) of Element 1: 1st p.v.	0.11	0.88*	0.07	0.11	−0.03	−0.04	0.04	−0.04	−0.19	0.14	−0.00
a–p	−0.06	0.02	−0.10	−0.04	0.00	−0.10	−0.03	0.92***	0.03	−0.02	−0.09
m–l	0.52	0.29	−0.03	−0.09	0.01	0.49	0.40	−0.19	−0.15	0.10	0.10
s–i	−0.59*	−0.06	−0.20	−0.10	−0.15	−0.32	−0.16	−0.49*	0.08	0.17	−0.03
Node 4 (l) of Element 2: 1st p.v.	−0.12	0.38	0.14	0.44	0.02	0.17	−0.51*	−0.22	−0.12	−0.31	−0.11
a–p	−0.14	0.03	−0.26	−0.62*	0.16	−0.06	−0.18	−0.14	0.37*	−0.07	0.30
m–l	0.01	0.05	0.02	0.03	0.17	−0.77***	0.23	0.09	−0.13	0.24	0.04
s–i	−0.05	−0.03	0.12	0.00	0.08	0.85***	0.13	0.04	−0.03	0.27	0.08
Node 7 (ast) of Element 2: 1st p.v.	0.17	0.69*	0.02	−0.10	−0.05	0.16	−0.27	0.11	0.10	−0.28	0.19
a–p	0.12	−0.01	−0.13	−0.07	0.17	0.09	−0.15	0.13	−0.26	0.77***	−0.10
m–l	0.01	0.07	−0.04	0.09	−0.05	−0.00	−0.04	−0.10	0.11	−0.16	0.92***
s–i	−0.27	−0.06	0.04	0.16	0.02	−0.11	0.29	−0.02	0.26	−0.10	−0.74***
Node 2 (fmt) of Element 3: 1st p.v.	0.00	−0.04	0.07	0.21	0.83***	−0.19	−0.22	0.14	−0.02	−0.01	0.01
a–p	−0.04	−0.36	−0.21	0.34	−0.33	−0.01	0.07	0.19	−0.58**	−0.12	0.18
m–l	0.08	0.06	0.00	−0.02	−0.02	−0.00	−0.84***	0.02	0.15	0.08	0.26
s–i	−0.06	0.17	0.02	−0.16	0.83***	0.13	0.29	−0.12	−0.02	0.14	−0.08
Node 5 (n) of Element 3: 1st p.v.	−0.14	0.26	0.80***	0.17	0.07	−0.06	0.07	0.08	0.03	−0.00	−0.24
a–p	−0.10	0.08	−0.74***	−0.09	0.00	−0.39	−0.01	0.04	−0.36*	0.04	−0.08
m–l	0.08	−0.22	0.02	0.07	−0.11	0.06	−0.11	0.10	0.86***	−0.01	0.01
s–i	−0.23	−0.25	0.74***	−0.23	0.08	−0.06	−0.18	−0.28	−0.23	0.07	0.10
Occlusal wear of UM1	−0.01	−0.08	0.16	0.12	−0.04	−0.02	0.12	−0.23	0.33	0.79***	−0.02

[1] The sample size is 35. The cumulative proportion of the variances of the eleven principal components is 83.50%.

[2] p.v.: principal value; a–p: direction cosine for the anterior-posterior axis; m–l: direction cosine for the medial-lateral axis; s–i: direction cosine for the superior-inferior axis.

* $P<0.05$; ** $P<0.01$; *** $P<0.001$, by a two-tailed bootstrap test.

Table 22. Principal component analysis of the correlations between the linearized first principal values and their direction cosines at six craniofacial landmarks, i.e., b, ba, l, ast, fmt, and n in the three right elements, and age in African-Americans.[1]

Variable[2]	Factor loadings										Total variance (%)
	PC I	II	III	IV	V	VI	VII	VIII	IX	X	
Node 3 (b) of Element 1: 1st p.v.	0.72***	0.12	0.07	0.17**	−0.14*	0.10	0.04	0.27***	0.17***	0.02	69.78
a–p	−0.24	0.11	−0.47	0.18	0.41	−0.04	−0.00	−0.08	−0.36	0.47*	84.85
m–l	−0.08	0.45	0.12	−0.42	−0.12	−0.46	−0.16	−0.14	0.44**	0.05	87.58
s–i	0.02	−0.66	0.30	0.16	−0.19	0.17	0.21	−0.10	0.00	−0.03	67.87
Node 4 (ba) of Element 1: 1st p.v.	0.60**	0.09	−0.19***	0.50***	0.03	0.13*	0.24***	0.25***	0.06	−0.10*	81.36
a–p	0.29	0.26	−0.33	0.07	0.63*	−0.28	−0.26	0.10	0.05	−0.20	86.02
m–l	−0.10	0.32	0.65	0.13	−0.13	−0.45**	0.24	−0.12	−0.07	0.02	85.77
s–i	−0.27	−0.39	−0.04	−0.63*	0.12	0.22	−0.04	0.10	0.21	0.32*	84.92
Node 4 (l) of Element 2: 1st p.v.	0.55*	0.12*	0.02	0.18***	−0.05	−0.28***	−0.26***	−0.12**	−0.16***	0.52***	81.56
a–p	−0.72***	−0.04	−0.19	0.19	0.49	0.12	−0.07	−0.06	0.12	0.01	86.94
m–l	0.14	0.64	0.46	−0.07	0.07	−0.17	0.00	0.26	−0.13	−0.00	76.10
s–i	0.12	−0.47	−0.46	−0.49	−0.28	−0.17	−0.08	0.18	0.04	−0.03	84.33
Node 7 (ast) of Element 2: 1st p.v.	0.51	−0.50***	0.11	0.23***	0.07	−0.40***	0.20***	−0.17**	0.05	0.29***	89.88
a–p	0.45*	0.09	0.29	−0.30	−0.33	0.30	−0.47*	−0.00	−0.34	0.03	91.99
m–l	0.30	−0.11	−0.55**	−0.21	0.04	−0.45**	0.48*	−0.09	0.12	−0.09	92.75
s–i	−0.59**	−0.04	0.43	0.50	0.07	0.08	0.01	−0.03	0.25*	0.02	85.51
Node 2 (fmt) of Element 3: 1st p.v.	0.46	0.08	0.17**	0.01	0.17**	0.37***	0.22***	0.27***	0.44***	0.21***	77.77
a–p	0.11	−0.46	0.06	0.37	0.12	−0.21	−0.42	−0.35	0.06	−0.29	80.34
m–l	−0.60***	0.03	−0.09	0.11	−0.15	−0.14	0.37	0.53**	−0.30*	0.09	93.60
s–i	0.25	0.60	−0.18	0.01	0.12	0.42	0.15	−0.42*	0.17	0.13	88.81
Node 5 (n) of Element 3: 1st p.v.	0.12	0.47**	−0.46**	0.03	−0.32*	0.10	0.24*	−0.18	−0.17	−0.28**	75.15
a–p	0.52**	−0.57	0.21	−0.01	0.25	0.10	0.21	−0.08	−0.20	−0.07	79.79
m–l	0.02	−0.06	0.56	−0.44	0.49	−0.17	0.21	0.16	−0.10	−0.13	88.33
s–i	−0.33	−0.08	−0.18	0.40	−0.61*	−0.20	−0.15	0.17	0.24	0.15	83.95
Age	0.25	−0.09	−0.14	0.21	0.20	−0.10	−0.41	0.59**	0.06	−0.08	70.40
Total contribution (%)	15.89	12.21	10.55	8.96	8.04	6.74	6.18	5.87	4.45	4.13	83.01
Cumulative proportion (%)	15.89	28.10	38.64	47.60	55.64	62.38	68.56	74.44	78.89	83.01	83.01

[1] The sample size is 27. The number of principal components shown here was determined so that the cumulative proportion of the variances of the principal components exceeded 80%.

[2] p.v.: principal value; a–p: direction cosine for the anterior-posterior axis; m–l: direction cosine for the medial-lateral axis; s–i: direction cosine for the superior-inferior axis.

* $P<0.05$; ** $P<0.01$; *** $P<0.001$, by a two-tailed bootstrap test.

Table 23. Rotated solution of the first ten principal components extracted from the correlations between the linearized first principal values and their direction cosines at six craniofacial landmarks, i.e., b, ba, l, ast, fmt, and n in the three right elements, and age in African-Americans.[1]

Variable[2]	Factor loadings									
	Fac I	II	III	IV	V	VI	VII	VIII	IX	X
Node 3 (b) of Element 1: 1st p.v.	0.35	−0.07	0.07	0.67*	−0.04	−0.12	−0.08	0.17	−0.25	0.00
a–p	−0.31*	0.16	−0.28	−0.20	0.06	0.02	0.20	−0.03	−0.04	0.75***
m–l	0.03	0.59*	0.53	−0.03	−0.11	−0.23	−0.24	−0.10	0.31	−0.12
s–i	−0.00	−0.77***	−0.04	0.01	−0.09	0.09	−0.04	−0.08	0.11	−0.21
Node 4 (ba) of Element 1: 1st p.v.	0.00	−0.15	−0.13	0.62*	−0.03	−0.12	0.01	0.17	−0.58**	0.09
a–p	−0.21	0.43**	−0.09	0.09	0.37	−0.20	−0.33	0.45**	−0.25	0.24
m–l	−0.02	−0.05	0.87*	−0.10	0.03	0.17	0.08	−0.15	−0.14	−0.02
s–i	−0.03	−0.03	−0.27	−0.03	0.12	−0.09	0.12	−0.07	0.85***	−0.07
Node 4 (l) of Element 2: 1st p.v.	0.39	−0.03	0.24	0.21	−0.13	−0.09	−0.26	0.10	−0.08	0.68***
a–p	−0.72***	0.18	−0.28	−0.29	0.04	0.35	0.03	0.03	0.16	0.07
m–l	0.24	0.38	0.57	0.17	0.28	0.22	0.20	0.10	−0.16	0.02
s–i	0.23	−0.09	−0.32	−0.15	−0.18	−0.66**	0.05	0.21	0.35	−0.15
Node 7 (ast) of Element 2: 1st p.v.	−0.02	−0.64**	0.26	0.22	−0.02	−0.35	−0.31	0.10	0.01	0.36*
a–p	0.92***	0.03	−0.06	0.02	0.10	0.20	−0.11	0.01	0.05	−0.02
m–l	−0.22	−0.02	−0.01	0.07	0.06	−0.92***	−0.01	−0.08	−0.12	0.06
s–i	−0.52***	−0.16	0.24	−0.07	−0.24	0.65***	0.01	−0.02	0.05	−0.14
Node 2 (fmt) of Element 3: 1st p.v.	0.01	−0.03	−0.02	0.85***	0.15	0.07	−0.00	−0.01	0.13	−0.04
a–p	−0.09	−0.36	−0.05	−0.28	−0.08	0.08	−0.69***	0.28	−0.15	−0.01
m–l	−0.30	−0.02	0.09	−0.25	−0.19	0.04	0.85***	0.16	−0.03	−0.01
s–i	0.02	0.42*	−0.15	0.40*	0.13	0.08	−0.19	−0.62***	−0.23	0.17
Node 5 (n) of Element 3: 1st p.v.	0.13	0.33	−0.18	−0.02	−0.12	−0.29	0.15	−0.38	−0.57**	−0.09
a–p	0.15	−0.69***	−0.10	0.18	0.44	−0.15	−0.18	0.07	−0.03	0.05
m–l	−0.04	−0.10	0.40	−0.01	0.75***	0.02	0.10	0.14	0.29	−0.17
s–i	−0.10	−0.02	0.07	−0.09	−0.88***	0.04	0.12	0.14	−0.01	−0.05
Age	0.06	0.09	−0.16	0.23	−0.03	0.02	−0.04	0.78***	−0.07	0.06

[1] The sample size is 27. The cumulative proportion of the variances of the ten principal components is 83.01%.

[2] p.v.: principal value; a–p: direction cosine for the anterior-posterior axis; m–l: direction cosine for the medial-lateral axis; s–i: direction cosine for the superior-inferior axis.

* $P<0.05$; ** $P<0.01$; *** $P<0.001$, by a two-tailed bootstrap test.

Table 24. Principal component analysis of the correlations between the linearized first principal values and their direction cosines at six craniofacial landmarks, i.e., b, ba, l, ast, fmt, and n in the three left elements, and age in African-Americans.[1]

Variable[2]	Factor loadings									Total variance (%)
	PC I	II	III	IV	V	VI	VII	VIII	IX	
Node 3 (b) of Element 1: 1st p.v.	0.67**	0.15*	0.14*	−0.22***	0.12*	0.07	−0.15**	0.17**	0.52***	88.04
a–p	0.19	−0.48	0.18	0.16	−0.50*	−0.00	0.09	−0.38	−0.23	77.57
m–l	0.06	0.04	0.13	−0.28	0.03	0.61*	−0.28	−0.49*	0.31	88.40
s–i	−0.09	0.72	−0.32	0.06	0.17	0.11	0.20	0.25	−0.17	80.26
Node 4 (ba) of Element 1: 1st p.v.	0.78***	0.08	0.22***	0.13*	0.01	0.27***	−0.06	0.19***	−0.25***	85.50
a–p	0.16	−0.02	−0.01	0.76*	−0.10	−0.00	0.03	−0.44*	0.15	83.05
m–l	0.35	−0.36	−0.50	−0.21	−0.17	0.22	0.29	0.14	−0.30	80.82
s–i	−0.38	0.54	0.17	−0.55*	0.18	0.04	0.14	0.07	−0.07	83.09
Node 4 (l) of Element 2: 1st p.v.	0.48	−0.05	0.33***	0.25***	0.51***	0.05	−0.43***	0.05	−0.13*	86.96
a–p	−0.31	−0.05	0.11	0.74*	0.34	−0.01	0.16	0.19	−0.04	83.85
m–l	−0.15	0.15	−0.05	−0.19	−0.45	0.53	0.32	0.05	0.29	75.11
s–i	0.14	−0.32	0.17	−0.52	−0.20	−0.57**	0.17	−0.21	−0.06	87.04
Node 7 (ast) of Element 2: 1st p.v.	0.64*	−0.45**	−0.04	−0.28**	0.27***	0.35***	0.01	0.20*	−0.12	93.08
a–p	0.17	0.17	0.58*	−0.23	0.17	−0.04	0.23	−0.06	−0.36	66.07
m–l	0.42*	0.18	−0.48	0.28	0.19	0.04	0.48*	0.00	0.17	81.28
s–i	−0.72***	0.21	0.22	0.09	−0.11	0.12	−0.44*	0.12	−0.01	85.68
Node 2 (fmt) of Element 3: 1st p.v.	0.47	0.47***	0.17**	0.01	−0.16**	−0.01	−0.23***	−0.32***	−0.31***	74.90
a–p	−0.44*	−0.08	0.06	−0.28	0.45	0.18	−0.05	−0.16	−0.24	59.49
m–l	0.23	0.53	−0.45	−0.25	0.20	−0.14	−0.08	−0.40**	0.12	83.64
s–i	0.09	−0.31	0.61	0.01	−0.34	−0.01	−0.01	0.45*	0.27	87.21
Node 5 (n) of Element 3: 1st p.v.	0.11	0.58***	0.24*	0.13	−0.44***	0.15	0.04	0.04	−0.26**	70.59
a–p	−0.21	−0.73	−0.17	−0.30	0.28	−0.01	−0.07	−0.02	0.00	77.44
m–l	−0.23	0.09	0.60	−0.05	0.11	0.30	0.48*	−0.15	0.00	78.09
s–i	0.19	0.42	−0.29	−0.23	−0.38	−0.23	−0.34	0.29	−0.04	74.23
Age	0.32	0.33	0.49*	−0.08	0.24	−0.45	0.30	−0.05	0.31*	90.94
Total contribution (%)	14.46	13.63	10.54	10.14	7.97	6.73	6.31	5.89	5.21	80.89
Cumulative proportion (%)	14.46	28.09	38.64	48.78	56.75	63.49	69.79	75.68	80.89	80.89

[1] The sample size is 27. The number of principal components shown here was determined so that the cumulative proportion of the variances of the principal components exceeded 80%.

[2] p.v.: principal value; a–p: direction cosine for the anterior-posterior axis; m–l: direction cosine for the medial-lateral axis; s–i: direction cosine for the superior-inferior axis.

* $P<0.05$; ** $P<0.01$; *** $P<0.001$, by a two-tailed bootstrap test.

Table 25. Rotated solution of the first nine principal components extracted from the correlations between the linearized first principal values and their direction cosines at six craniofacial landmarks, i.e., b, ba, l, ast, fmt, and n in the three left elements, and age in African-Americans.[1]

Variable[2]	Factor loadings								
	Fac I	II	III	IV	V	VI	VII	VIII	IX
Node 3 (b) of Element 1: 1st p.v.	0.16	0.05	−0.24	−0.08	−0.09	0.39	0.30	0.12	0.72***
a–p	−0.06	−0.49	0.13	0.56*	−0.12	0.06	0.18	0.25	−0.30
m–l	−0.05	0.03	0.15	0.02	0.00	0.92***	−0.02	−0.10	−0.00
s–i	−0.16	0.50	−0.03	−0.36	−0.36	−0.26	−0.00	−0.44*	0.04
Node 4 (ba) of Element 1: 1st p.v.	0.39	0.12	0.01	0.09	−0.49	0.11	0.60*	0.19	0.16
a–p	0.07	0.17	0.09	0.86**	−0.14	0.00	−0.13	−0.14	0.05
m–l	−0.24	−0.12	−0.16	0.01	0.09	−0.10	0.78***	−0.07	−0.28
s–i	−0.18	−0.00	0.27	−0.76**	−0.16	0.06	−0.27	−0.21	0.08
Node 4 (l) of Element 2: 1st p.v.	0.85***	0.20	0.05	0.09	−0.08	0.15	0.16	0.11	0.17
a–p	0.18	0.56*	0.31	0.31	0.15	−0.46*	−0.24	0.11	−0.07
m–l	−0.74***	0.16	0.08	−0.08	−0.16	0.32	0.09	0.15	−0.01
s–i	−0.03	−0.89***	0.01	−0.10	0.15	−0.13	0.06	0.04	0.16
Node 7 (ast) of Element 2: 1st p.v.	0.30	−0.02	0.01	−0.10	0.19	0.24	0.84***	0.17	0.05
a–p	0.26	−0.26	0.53*	−0.29	−0.34	−0.06	0.09	0.07	0.13
m–l	−0.19	0.33	−0.02	0.28	−0.01	−0.23	0.46**	−0.45*	0.35
s–i	−0.02	0.26	−0.05	−0.24	−0.05	0.12	−0.72***	0.24	−0.36*
Node 2 (fmt) of Element 3: 1st p.v.	0.31	−0.19	−0.05	0.08	−0.71**	0.21	0.04	−0.24	0.04
a–p	0.16	0.03	0.37	−0.38	0.31	0.14	−0.14	−0.19	−0.33
m–l	0.00	−0.05	−0.24	−0.11	−0.13	0.20	−0.01	−0.80***	0.26
s–i	−0.04	−0.11	0.02	0.01	−0.03	0.00	−0.01	0.89***	0.26
Node 5 (n) of Element 3: 1st p.v.	−0.14	0.08	0.04	−0.04	−0.82***	−0.01	−0.08	0.07	−0.04
a–p	0.09	−0.22	0.02	−0.10	0.77***	0.07	0.17	0.08	−0.27*
m–l	−0.19	0.03	0.81***	−0.11	−0.12	0.10	−0.11	0.17	0.09
s–i	−0.08	−0.08	−0.69***	−0.28	−0.40*	−0.06	−0.02	−0.06	0.07
Age	0.16	−0.22	0.29	−0.06	−0.17	−0.16	−0.13	−0.05	0.82***

[1] The sample size is 27. The cumulative proportion of the variances of the nine principal components is 80.89%.
[2] p.v.: principal value; a–p: direction cosine for the anterior-posterior axis; m–l: direction cosine for the medial-lateral axis; s–i: direction cosine for the superior-inferior axis.
* $P<0.05$; ** $P<0.01$; *** $P<0.001$, by a two-tailed bootstrap test.

Table 26. Kendall's rank correlation coefficients between the right and left sides of three samples in the variation pattern of factor loadings on the principal components and rotated factors obtained from the first set of neurocranial landmarks (ft, STH, i, SCH, g, and zm) and dental wear or age.[1]

				1	2	3	4	5	6	7	8	9	10	11	12
1	Japanese	Right	PC IV	—											
2			Fac VIII	.35*	—										
3		Left	PC VIII	—	—	—									
4			Fac VIII	—	—	.51***	—								
5	Indians	Right	PC I	—	—	—	.38**	—							
6			Fac IX	—	—	—	—	—	—						
7		Left	PC III	—	—	—	—	—	—	—					
8			Fac IV	.35*	—	—	—	.42**	—	—	—				
9	African-Americans	Right	PC II	—	—	—	—	—	—	—	—	—			
10			Fac II	—	—	—	—	.32*	—	—	.31*	.51***	—		
11		Left	PC VII	.31*	—	—	—	—	—	—	—	—	—	—	
12			Fac IX	—	—	—	—	—	—	—	—	.45**	.53***	—	—

[1]The principal components and rotated factors that were superficially most highly correlated with dental wear or age in each analysis were compared with one another. Only those rank correlation coefficients significant at the 5% level are listed here. The signs of rank correlation coefficients are removed because the signs of factor loadings are reversible. The original factor loadings are listed in Tables 2 to 13.

* $P<0.05$; ** $P<0.01$; *** $P<0.001$, by a two-tailed test.

Table 27. Kendall's rank correlation coefficients between the right and left sides of three samples in the variation pattern of factor loadings on the principal components and rotated factors obtained from the second set of neurocranial landmarks (b, ba, l, ast, fmt, and n) and dental wear or age.[1]

				1	2	3	4	5	6	7	8	9	10	11	12
1	Japanese	Right	PC IV	—											
2			Fac IV	.53***	—										
3		Left	PC VIII	—	—	—									
4			Fac VIII	—	—	—	—								
5	Indians	Right	PC V	—	—	—	—	—							
6			Fac VI	—	—	—	—	.32*	—						
7		Left	PC III	—	—	—	—	—	.37*	—					
8			Fac X	—	—	.28*	—	—	—	.28*	—				
9	African-Americans	Right	PC VIII	.33*	—	—	—	—	—	—	.29*	—			
10			Fac VIII	—	—	—	—	—	—	—	—	.46**	—		
11		Left	PC III	.35*	—	—	—	—	.42**	.32*	—	—	—	—	
12			Fac IX	.30*	—	—	—	—	—	—	—	.30*	—	—	—

[1]The principal components and rotated factors that were superficially most highly correlated with dental wear or age in each analysis were compared with one another. Only those rank correlation coefficients significant at the 5% level are listed here. The signs of rank correlation coefficients are removed because the signs of factor loadings are reversible. The original factor loadings are listed in Tables 14 to 25.

* $P<0.05$; ** $P<0.01$; *** $P<0.001$, by a two-tailed test.

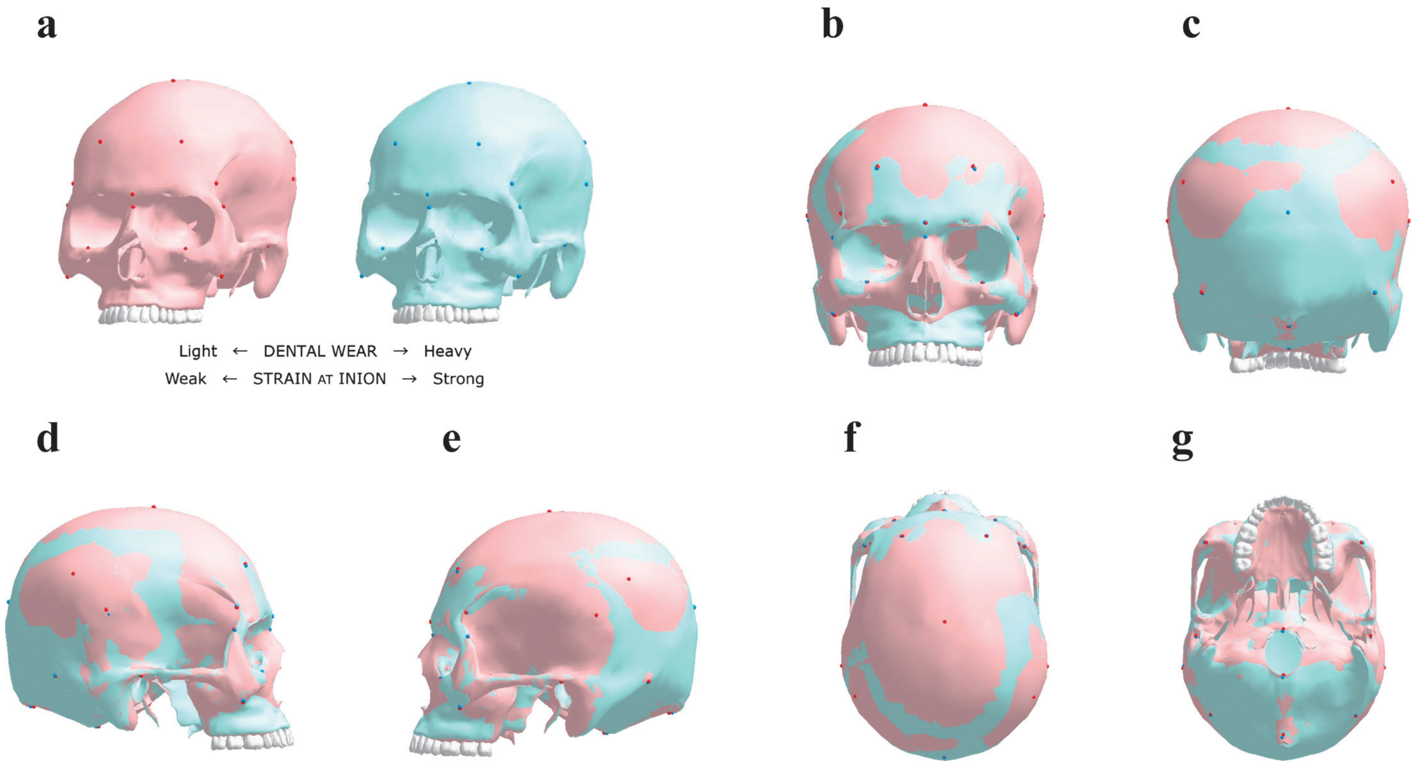

Fig. 2. Two crania of early modern Japanese males, Nos. 10013 and 10078, superimposed in the original coordinate system, where the origin is set at the foot of the perpendicular from bregma to the line segment, nasion-lambda. Each of these crania is one of the five lowest or five highest extremes in the scores of the PCs which are significantly correlated with both the degree of occlusal wear on the UM1 and the first principal value at the inion (Tables 2 and 4). Only the form in the neighborhood of the landmarks analyzed is reliable because far regions off the landmarks are manually deformed from a template with Rokkaku-Daiou Super 6. **a.** No. 10013 (left) and No. 10078 (right). **b.** Anterior view of superimposed crania. **c.** Posterior view. **d.** Lateral view from the right. **e.** Lateral view from the left. **f.** Superior view. **g.** Inferior view.

Table 28. Principal components from two correlation matrices on the linearized first principal values and their direction cosines at basion and the degree of occlusal wear on the maxillary first molar.[1]

Variable[2]		Factor loadings	
		PC III from right elemens	PC VI from left elements
Node 4 (ba) of Element 1:	1st p.v.	0.08	0.06
	a–p	−0.30	0.06
	m–l	0.77**	0.09
	s–i	−0.32	−0.02
Node 2 (ba) of Element 2:	1st p.v.	0.01	−0.20***
	a–p	−0.18	−0.25
	m–l	0.40	−0.00
	s–i	0.17	0.49
Node 8 (ba) of Element 3:	1st p.v.	−0.32**	0.03
	a–p	0.18	−0.10
	m–l	0.26	0.47
	s–i	0.07	−0.02
Occlusal wear of UM1		−0.59***	0.64***

[1] The sample consists of 33 skulls of early modern Japanese males (the first data set). The two PCs shown here were extracted from two correlation matrices on only two landmarks, basion and porion, for the right and left sides, respectively. Each of basion and porion is one of the eight nodes of each of three elements on either side of the skull. Both PCs are most highly correlated with dental wear among the PCs obtained from the respective correlation matrices.

[2] p.v.: principal value; a–p: direction cosine for the anterior-posterior axis; m–l: direction cosine for the medial-lateral axis; s–i: direction cosine for the superior-inferior axis.

* $P<0.05$; ** $P<0.01$; *** $P<0.001$, by a two-tailed bootstrap test.

broader facial region (Fig. 1). The remarkable findings, particularly from the viewpoint of repeatability between the results on the right and left sides, are 1) a significant positive association between the degree of dental wear and the magnitude of strain at the inion in Japanese (Tables 2 and 4; Fig. 2); 2) a significant inverse association between the degree of dental wear and the magnitude of strain at the frontotemporale in Japanese (Tables 2 and 4); 3) a significant positive association between age and the magnitude of strain at the center of the parietal tuber in African-Americans (Tables 11 and 13); and 4) significant positive and inverse associations of the degree of dental wear with the magnitude of strain at the frontomalare temporale and asterion, respectively, in Japanese (Tables 14 and 16).

As stated above, the details indicated by previous and the present FESAs of the same Japanese sample are not necessarily consistent. Besides, the results from the three samples examined here did not necessarily show similar tendencies at least regarding the associations with dental wear or age. Although the latter discrepancies are due possibly to some between-population differences in genetic and environmental factors, the former is considered to be caused, in part, by the approach to selecting landmarks in constructing an element or hexahedron in the skull. Namely, a landmark common to some different elements may show different tendencies in its principal value and direction cosines according to the elements selected. In Table 28, patterns of variation in factor loadings are shown for the 3D strain variables at a landmark, the basion, in six different elements. These patterns of variation reveal no clear consistency between different elements. Comparing with Tables 14 and 16, however, it can be found that the patterns of variation in factor loadings for Node 4 (ba) of Element 1 of both sides (PC IV in Table 14 and PC VIII in Table 16) are very similar to those (right PC III and left PC VI) shown in Table 28, even though the combination of variables to be used in PCAs differs. This suggests that 3D strain properties of each cranial local region are specific. In sum, when we obtain some information on a landmark by FESM, we should interpret it while keeping in mind the whole structure of the element to which the landmark in question belongs.

Interpreting the results of the present study in such a way, the following inferences may be possible.

1) If the degree of dental wear is merely an indicator of age, PC IV in Table 2 and PC VIII in Table 4 imply that the magnitude of strain in the neighborhood of the inion increases with age in Japanese. This may indicate greater variation in the development of the nuchal muscles in older people. Alternatively, if the degree of dental wear is due mainly to the extent of occlusal force and if the masticatory and nuchal muscles are considerably controlled by common genetic and/or environmental factors, it may be inferred that people with powerful skeletal muscles tend to have greater structural variation around the posterior end of the nuchal plane. At least, this finding is not considered an artificial phenomenon because the intra-observer errors for the principal value at the inion are fairly low (Table 1). Zafar *et al.* (2000) suggested on the basis of physiological experiments that functional jaw movements comprise concomitant mandibular and head-neck movements involving the temporomandibular, the atlanto-occipital, and the cervical spine joints, and are caused by jointly activated jaw and neck muscles. If so, the strong association between the inion and dental wear found in the present study may also partly be explained by this combination of mandibular and head-neck movements.

2) Similarly, both PC VIIIs in Tables 2 and 4 suggest that the magnitude of strain in the neighborhood of the frontotemporale decreases with age in Japanese, or tends to be smaller in individuals with stronger masticatory force. In any case, this phenomenon seems to be associated with the development of the temporalis muscle. As the intra-observer errors for the principal value at the frontotemporale are relatively low (Table 1), this finding seems reliable.

3) Fac II in Table 11 and Fac IX in Table 13 clearly show that the magnitude of strain at the center of the parietal tuber (SCH) increases with age in African-Americans. As the intra-observer errors for the principal value at SCH are relatively low (Table 1), this finding seems to be a biological phenomenon associated with aging. As shown in Table 11, however, age is not only positively associated with the principal value at SCH but also inversely related with its direction cosine for the medial-lateral axis. If this is correct, it means that the center of the right parietal tuber tends to shift to the right side or laterally with age. However, the intra-observer errors in the direction cosine for the medial-lateral axis at SCH are very high (Table 1), and, furthermore, in the left parietal tuber, there is no similar tendency (Table 13). Therefore, it may be safe to say that, at least, the magnitude of strain at the center of the parietal tuber increases with age regardless of the direction. Mizoguchi (1992), using another sample from early modern Japanese males, suggested that individuals with heavier dental wear have smaller inter-parietal-tuber breadth, smaller basibregmatic height, and greater bizygomatic breadth. The finding on SCH in the present study is not necessarily inconsistent with this suggestion by Mizoguchi (1992). Finally, it should be furthermore considered that the rate of admixture with other populations may be different from generation to generation in the United States. If so, this may also influence the association between the magnitude of strain at SCH and age.

4) PC IV in Table 14 and PC VIII in Table 16 imply that the magnitude of strain at the frontomalare temporale increases with age and, simultaneously, the magnitude of strain at the asterion decreases with age in Japanese, or the magnitude of strain tends to be larger at the frontomalare temporale and smaller at the asterion in individuals with stronger masticatory force. However, while the intra-observer error in the principal value at the right asterion is relatively low, those for the left asterion and the right and left frontomalare temporale are very high (Table 1). Therefore, it is difficult from these findings to make any meaningful argument.

Finally, from the present and previous findings, it can be said at least that the craniofacial form varies along with age even in adulthood and, possibly, also in response to mechanical stresses from the masticatory and/or nuchal muscles.

Interrelationship between 3D structural strains

In the above section, the focus of attention was the association between 3D structural strain and dental wear or age. Apart from this, however, the results of the present analyses further suggest some other strong associations in the magnitude of strain between several cranial landmarks across the three samples. For example, strong associations between the principal values at the bregma, basion, and lambda are indicated by two PC IIs from Japanese (Tables 14 and 16), Fac III from Indians (Table 19), and PC I from African-Americans (Table 22). In addition to these, Fac IIs from Japanese (Table 15) and Indians (Table 21), and Fac IV (Table 23) and PC I (Table 24) from African-Americans also show the strong association between the bregma and basion. Although the causes of these strong associations cannot be determined here because there are no data on candidate factors, one of the possible causes is the structural variation in height of the brain.

To determine the causes of such interrelationships between sub-structures of the skull, we should make every effort to collect a range of information on environmental factors together with skeletal materials.

Summary and Conclusions

In order to explore the possibility that the masticatory force and/or aging are causes of part of the morphological variation in the human skull, finite element scaling analysis (FESA) was carried out using three male adult samples from early modern Japanese, Indians, and African-Americans. Principal component analyses and the rotated solutions of the 3D structural deviations obtained by FESAs suggested that the magnitude of strain in the neighborhood of the inion increases with age in Japanese, or that people with powerful skeletal muscles tend to have greater structural variation around the posterior end of the nuchal plane; and that the magnitude of strain in the neighborhood of the frontotemporale decreases with age in Japanese, or tends to be smaller in individuals with stronger masticatory force. It was clearly shown that the magnitude of strain at the center of the parietal tuber increases with age in African-Americans. In addition to these findings, strong associations in the magnitude of strain were also found between several landmarks such as bregma, basion, and lambda across the three samples.

At present, it can be said at least that the craniofacial form varies along with age even in adulthood and, possibly, also in response to mechanical stresses from the masticatory and/or nuchal muscles. In the future, data on other possible causes than dental wear, age, sex, and so on should also be collected.

Acknowledgments

I would like to thank the late Professors Hisashi Suzuki and Kazuro Hanihara of the University of Tokyo, Dr. Douglas H. Ubelaker of the Smithsonian Institution, and Emeritus Professor Eisaku Kanazawa of Nihon University for their granting of access to the skeletal collections of their universities or institutions. I am also thankful to Dr. Makiko Kouchi of National Institute of Advanced Industrial Science and Technology, Tokyo, for helpful suggestions and comments, and, furthermore, to Salford Software Ltd. and "kito" for kindly providing their very useful software, FTN77 and CPad, respectively, via the Internet. In addition, I am grateful to Mr. Fahim Fazli for uploading a useful free 3D model of the human skull onto the Internet.

This work was partly supported by a Grant-in-Aid for Scientific Research (C) from the Japan Society for the Promotion of Science (Project No. 22570224). The manuscript was copyedited by Medical English Service, Kyoto.

Literature Cited

Asano, C., 1971. *Inshi-Bunsekiho-Tsuron (Outlines of Factor Analysis Methods)*. Kyoritsu-Shuppan, Tokyo. (In Japanese.)

Bathe, K.-J., and E. L. Wilson, 1976. *Numerical Methods in Finite Element Analysis.* Prentice-Hall, Englewood

Cliffs.

Bienvenu, T., F. Guy, W. Coudyzer, E. Gillissen, G. Roualdes, P. Vignaud, and M. Brunet, 2011. Assessing endocranial variations in great apes and humans using 3D data from virtual endocasts. *American Journal of Physical Anthropology*, **145**: 231–246.

Bigoni, L., J. Veleminska, and J. Bruzek, 2010. Three-dimensional geometric morphometric analysis of cranio-facial sexual dimorphism in a Central European sample of known sex. *Homo*, **61**: 16–32.

Bookstein, F. L. 1991. *Morphometric Tools for Landmark Data: Geometry and Biology.* Cambridge University Press, Cambridge.

Bookstein, F. L., P. Gunz, P. Mitteroecker, H. Prossinger, K. Schaefer, and H. Seidler, 2003. Cranial integration in *Homo*: singular strains analysis of the midsagittal plane in ontogeny and evolution. *Journal of Human Evolution*, **44**: 167–187.

Cavalli-Sforza, L. L., and W. F. Bodmer, 1971. *The Genetics of Human Populations.* W. H. Freeman and Company, San Francisco.

Cheverud, J. M., L. A. P. Kohn, L. W. Konigsberg, and S. R. Leigh, 1992. Effects of fronto-occipital artificial cranial vault modification on the cranial base and face. *American Journal of Physical Anthropology*, **88**: 323–345.

Cheverud, J., J. L. Lewis, W. Bachrach, and W. D. Lew, 1983. The measurement of form and variation in form: An application of three-dimensional quantitative morphology by finite-element methods. *American Journal of Physical Anthropology*, **62**: 151–165.

Cheverud, J. M., and J. T. Richtsmeier, 1986. Finite-element scaling applied to sexual dimorphism in rhesus macaque (*Macaca mulatta*) facial growth. *Systematic Zoology*, **35**: 381–399.

Coquerelle, M., F. L. Bookstein, J. Braga, D. J. Halazonetis, G. W. Weber, and P. Mitteroecker, 2011. Sexual dimorphism of the human mandible and its association with dental development. *American Journal of Physical Anthropology*, **145**: 192–202.

Detroit, F., 2000. The period of transition between *Homo erectus* and *Homo sapiens* in East and Southeast Asia: New perspectives by the way of geometric morphometrics. *Acta Anthropologica Sinica*, Suppl. to Vol. **19**: 62–68.

Diaconis, P., and B. Efron, 1983. Computer-intensive methods in statistics. *Scientific American*, **248**: 96–108, 138.

Efron, B., 1979a. Bootstrap methods: Another look at the jackknife. *Annals of Statistics*, **7**: 1–26.

Efron, B., 1979b. Computers and the theory of statistics: Thinking the unthinkable. *SIAM Review*, **21**: 460–480.

Efron, B., 1982. *The Jackknife, the Bootstrap and Other Resampling Plans*. Society for Industrial and Applied Mathematics, Philadelphia.

Freidline, S. E., P. Gunz, I. Jankovic, K. Harvati, and J.-J. Hublin, 2012. A comprehensive morphometric analysis of the frontal and zygomatic bone of the Zuttiyeh fossil from Israel. *Journal of Human Evolution*, **62**: 225–241.

Fukumoto, I., and O. Kondo, 2010. Three-dimensional craniofacial variation and occlusal wear severity among inhabitants of Hokkaido: comparisons of Okhotsk culture people and the Ainu. *Anthropological Science*, **118**: 161–172.

Gonzalez, P. N., V. Bernal, and S. I. Perez, 2011. Analysis of sexual dimorphism of craniofacial traits using geometric morphometric techniques. *International Journal of Osteoarchaeology*, **21**: 82–91.

Gunz, P., and K. Harvati, 2007. The Neanderthal "chignon": Variation, integration, and homology. *Journal of Human Evolution*, **52**: 262–274.

Gunz, P., P. Mitteroecker, S. Neubauer, G. W. Weber, and F.L. Bookstein, 2009. Principles for the virtual reconstruction of hominin crania. *Journal of Human Evolution*, **57**: 48–62.

Harvati, K., 2003. The Neanderthal taxonomic position: models of intra- and inter-specific craniofacial variation. *Journal of Human Evolution*, **44**: 107–132.

Harvati, K., J. J. Hublin, and P. Gunz, 2010. Evolution of middle-late Pleistocene human cranio-facial form: A 3D approach. *Journal of Human Evolution*, **59**: 445–464.

Hennessy, R. J., and C. B. Stringer, 2002. Geometric morphometric study of the regional variation of modern human craniofacial form. *American Journal of Physical Anthropology*, **117**: 37–48.

Hublin, J.-J., D. Weston, P. Gunz, M. Richards, W. Roebroeks, J. Glimmerveen, and L. Anthonis, 2009. Out of the North Sea: the Zeeland Ridges Neandertal. *Journal of Human Evolution*, **57**: 777–785.

Kohn, L. A. P., S. R. Leigh, S. C. Jacobs, and J. M. Cheverud, 1993. Effects of annular cranial vault modification on the cranial base and face. *American Journal of Physical Anthropology*, **90**: 147–168.

Kohn, L. A. P., S. R. Leigh, and J. M. Cheverud, 1995. Asymmetric vault modification in Hopi crania. *American Journal of Physical Anthropology*, **98**: 173–195.

Lawley, D. N., and A. E. Maxwell, 1963. *Factor Analysis as a Statistical Method*. Butterworth, London. (Translated by M. Okamoto, 1970, into Japanese and entitled *Inshi-Bunsekiho*. Nikkagiren, Tokyo.)

Leigh, S. R., and J. M. Cheverud, 1991. Sexual dimorphism in the baboon facial skeleton. *American Journal of Physical Anthropology*, **84**: 193–208.

Lewis, J. L., W. D. Lew, and J. R. Zimmerman, 1980. A nonhomogeneous anthropometric scaling method based on finite element principles. *Journal of Biomechanics*, **13**: 815–824.

Lundström, A., 1948. *Tooth Size and Occlusion in Twins.* S. Karger, Basle.

Malvern, L.E., 1969. *Introduction to the Mechanics of a Continuous Medium.* Prentice-Hall, Englewood Cliffs.

Marcus, L. F., M. Corti, A. Loy, G. J. P. Naylor, and D. E. Slice (eds.), 1996. *Advances in Morphometrics*. Plenum Press, New York.

Martin, R., and K. Saller, 1957. *Lehrbuch der Anthropologie*, dritte Aufl., Bd. I. Gustav Fischer Verlag, Stuttgart.

Matsukawa, S., 2002. Three dimensional morphological analysis of sexual dimorphism in modern Japanese hip bones by means of FESA and EDMA. *Anthropological Science (Japanese Series)*, **109**: 101–118. (In Japanese with English summary.)

Makishima, H., and N. Ogihara, 2009. Three-dimensional geometric morphometric study of craniofacial variations in Jomon populations. *Anthropological Science (Japanese Series)*, **117**: 11–21. (In Japanese with English summary.)

Mine, K., and T. Ogata, 1989. Coordinate transformation of the cranial landmarks using shape functions. *Acta Anatomica Nipponica*, **64**: 368. (In Japanese.)

Mizoguchi, Y., 1977. Genetic variability of permanent tooth crowns as ascertained from twin data. *Journal of Anthropological Society of Nippon*, **85**: 301–309.

Mizoguchi, Y., 1992. Poor swelling of the parietal tuber associated with the strong occlusal wear of the maxillary first molar. *Bulletin of the National Science Museum, Tokyo, Series D*, **18**: 39–62.

Mizoguchi, Y., 1993. Overall associations between dental size and foodstuff intakes in modern human populations. *Homo*, **44**: 37–73.

Mizoguchi, Y., 2000a. Relations between the three-dimensional structural variations at cranial landmarks estimated by finite element scaling analysis and the degree of dental wear. *Anthropological Science*, **108**: 135.

Mizoguchi, Y., 2000b. Analysis of three-dimensional variations in the skull by the use of finite element scaling method. In: *Summary of Presented Papers at the Tenth Meeting of Japan Society for Archaeological Information*, pp. 19–24. Japan Society for Archaeological Information, Tokyo. (In Japanese.)

Mizoguchi, Y., 2004. Associations between the neurocranium and the foot bones: Toward the solution of the brachycephalization problem. *Bulletin of the National Science Museum, Tokyo, Series D*, **30**: 9–36.

Mizoguchi, Y., 2005. Associations between 3D structural deviations in the neighborhood of cranial landmarks and the degree of dental wear. In: Zadzinska, E. (ed.), *Current Trends in Dental Morphology Research*, pp. 105–114. University of Lodz Press, Lodz.

Neubauer, S., P. Gunz, and J.-J. Hublin, 2010. Endocranial shape changes during growth in chimpanzees and humans: A morphometric analysis of unique and shared aspects. *Journal of Human Evolution*, **59**: 555–566.

Noback, M. L., K. Harvati, and F. Spoor, 2011. Climate-related variation of the human nasal cavity. *American Journal of Physical Anthropology*, **145**: 599–614.

Okuno, T., T. Haga, K. Yajima, C. Okuno, S. Hashimoto, and Y. Furukawa, 1976. *Zoku-Tahenryo-Kaisekiho* (*Multivariate Analysis Methods, Part 2*). Nikkagiren, Tokyo. (In Japanese.)

Okuno, T., H. Kume, T. Haga, and T. Yoshizawa, 1971. *Tahenryo-Kaisekiho* (*Multivariate Analysis Methods*). Nikkagiren, Tokyo. (In Japanese.)

Richtsmeier, J.T., 1987. Comparative study of normal, Crouzon, and Apert craniofacial morphology using finite element scaling analysis. *American Journal of Physical Anthropology*, **74**: 473–493.

Richtsmeier, J. T., and A. Walker, 1993. A morphometric study of facial growth. In: Walker, A., and R. E. Leakey (eds.), *The Nariokotome.* Homo erectus *skeleton*, pp. 391–410. Harvard University Press, Cambridge.

Siegel, S., 1956. *Nonparametric Statistics for the Behavioral Sciences*. McGraw-Hill Kogakusha, Tokyo.

Singh, N., K. Harvati, J. J. Hublin, and C. P. Klingenberg, 2012. Morphological evolution through integration: A quantitative study of cranial integration in *Homo*, *Pan*, *Gorilla* and *Pongo*. *Journal of Human Evolution*, **62**: 155–164.

Slice, D. E., 2005. Modern Morphometrics. In: D. E. Slice (ed.), *Modern Morphometrics in Physical Anthropology*, pp. 1–45. Kluwer Academic/Plenum Publishers, New York.

Takeuchi, K., and H. Yanai, 1972. *Tahenryo-Kaiseki no Kiso* (*A Basis of Multivariate Analysis*). Toyokeizai-Shinposha, Tokyo. (In Japanese.)

von Cramon-Taubadel, N., 2011. The relative efficacy of functional and developmental cranial modules for reconstructing global human population history. *American Journal of Physical Anthropology*, **146**: 83–93.

von Cramon-Taubadel, N., and H. F. Smith, 2012. The relative congruence of cranial and genetic estimates of hominoid taxon relationships: Implications for the reconstruction of hominin phylogeny. *Journal of Human Evolution*, **62**: 640–653.

Weisensee, K. E., and R. L. Jantz, 2011. Secular changes in craniofacial morphology of the Portuguese using geometric morphometrics. *American Journal of Physical Anthropology*, **145**: 548–559.

Williams, S. E., and D. E. Slice, 2010. Regional shape change in adult facial bone curvature with age. *American Journal of Physical Anthropology*, **143**: 437–447.

Yasuda, S., 1969. *Shakai-Tokeigaku (Social Statistics)*. Maruzen, Tokyo. (In Japanese.)

Zafar, H., E. Nordh, and P.-O. Eriksson, 2000. Temporal coordination between mandibular and head-neck movements during jaw opening-closing tasks in man. *Archives of Oral Biology*, **45**: 675–682.